

Controls on the strength of coupling among climate, erosion, and deformation in two-sided, frictional orogenic wedges at steady state

K. X. Whipple and B. J. Meade

Department of Earth, Atmospheric and Planetary Sciences, Massachusetts Institute of Technology, Cambridge, Massachusetts, USA

Received 6 January 2003; revised 7 December 2003; accepted 29 December 2003; published 5 March 2004.

[1] Many important insights regarding the coupling among climate, erosion, and tectonics have come from numerical simulations using coupled tectonic and surface process models. However, analyses to date have left the strength of the coupling between climate and tectonics uncertain and many questions unanswered. We present an approximate analytical solution for two-sided orogenic wedges obeying a frictional rheology, and in a condition of flux steady state, that makes explicit the nature and sensitivity of the coupling between climate and deformation. We make the simplifying assumption that the wedge grows in a self-similar fashion consistent with Airy isostasy such that topographic taper is invariant with orogen width, tectonic influx rate, and climate. We illustrate first how and why the form of the erosion rule matters to orogen evolution and then derive a physically based orogen-scale erosion rule. We show that steady state orogen width, crest elevation, and crustal thickness are controlled by the ratio of accretionary flux to erosional efficiency to a power dictated by the erosion process. Remarkably, we show that for most combinations of parameters in the erosion law, rock uplift rate is more strongly controlled by erosional efficiency than it is by the accretionary flux. Further, assuming frontal accretion with no underplating, the spatial distribution of erosional efficiency dictates the relative rock uplift rates on the pro-wedge and retro-wedge and the time-averaged trajectories of rocks through the orogen. The restriction to invariant frictional properties is conservative in these respects; systems subject to positive feedback between erosion and rheology will exhibit even stronger coupling among climate, erosion, and deformation than shown here. *INDEX TERMS*: 1815 Hydrology: Erosion and sedimentation; 1824 Hydrology: Geomorphology (1625); 8102 Tectonophysics: Continental contractional orogenic belts; 8107 Tectonophysics: Continental neotectonics; 8120 Tectonophysics: Dynamics of lithosphere and mantle—general; *KEYWORDS*: erosion, rock uplift, critical taper, orogen evolution, stream power

Citation: Whipple, K. X., and B. J. Meade (2004), Controls on the strength of coupling among climate, erosion, and deformation in two-sided, frictional orogenic wedges at steady state, *J. Geophys. Res.*, 109, F01011, doi:10.1029/2003JF000019.

1. Motivation

[2] The recognition of a dynamic coupling among climate, erosion, and tectonics that plays a first-order role in orogen evolution is arguably one of the most interesting geoscience discoveries in the last 20 years. Numerical simulations using coupled tectonic and surface process models [e.g., *Avouac and Burov*, 1996; *Beaumont et al.*, 1992, 1996, 2001; *Koons*, 1989, 1995; *Koons et al.*, 2002; *Willett*, 1999a] have clearly demonstrated that the geodynamics of active orogens is powerfully influenced by the surface boundary conditions. The efficiency of erosion, and its concentration on windward slopes, has been shown to govern steady state orogen width, surface rock uplift rates, and strain partitioning within the orogen [e.g.,

Beaumont et al., 1992; *Beaumont et al.*, 1996; *Willett*, 1999a]. Topographic and thermochronologic data from Taiwan's Central Range, New Zealand's Southern Alps, the Olympics, and the Andes support these findings [*Batt et al.*, 1999, 2000; *Beaumont et al.*, 1996; *Koons*, 1995; *Montgomery et al.*, 2001; *Willett and Brandon*, 2002; *Willett et al.*, 2001]. Indeed, the dramatic along-strike variability in orogen width, depth of exhumation, and rock uplift rate that characterize the Andes has been attributed to along-strike differences in climate [*Dahlen and Suppe*, 1988; *Horton*, 1999; *Masek et al.*, 1994; *Montgomery et al.*, 2001].

[3] An implication of these models and data is that at orogen scale, rock uplift rate is dictated by the erosion rate rather than vice versa, as is commonly assumed [e.g., *Howard*, 1980; *Whipple and Tucker*, 1999; *Willgoose et al.*, 1991]. However, analyses to date have left the strength of the coupling and feedback between climate

and tectonics uncertain and many questions unanswered. For example, given a change in erosional efficiency (say, related to an increase in mean annual precipitation or the frequency of large storms), how much does rock uplift rate increase in response? How is the change in rock uplift rate induced? Is rock uplift rate more strongly controlled by erosional efficiency or by accretionary flux? What is the influence of the efficiency of recycling of sediment deposited in the foreland back into the orogen? Is it necessary to always use fully coupled models, or can the fundamental characteristics of the dynamic feedbacks among climate, erosion, and tectonics be established in simple, general, and quantitative terms? In addition, it has remained unclear whether the details of the erosion processes are important to the geodynamic evolution of the orogen and if so, how they come into play. Perhaps it is for these reasons that geomorphologists commonly treat uplift as an independent variable, often driving models with “uniform block uplift” [e.g., Howard, 1994; Tucker, 1996; Whipple and Tucker, 1999; Willgoose et al., 1991]. Although this can be a useful device for exploring aspects of landscape evolution, its prevalence as a model boundary condition suggests that the implications of recent work with coupled tectonic and surface process models have not been fully appreciated.

2. Approach and Scope

[4] The goal of this paper is to elucidate the essential nature of the interactions between climate-driven erosion and tectonics. To achieve this goal, we pursue an approximate analytical solution such that the various controls on system behavior and the sensitivity of the coupling between erosional efficiency and rock uplift rate, for instance, can be explicitly stated. Simplifications are made to allow this analytical formulation. We restrict our analysis to two-sided orogenic wedges obeying a frictional rheology and in a condition of flux steady state [Willett and Brandon, 2002]. We focus on the idealized steady state condition in order to draw out the fundamental aspects of the problem, not because we believe that this condition is commonly attained in nature. The mechanics of frictional orogenic wedges predict the development and maintenance of a critical taper geometry [e.g., Dahlen, 1984; Davis et al., 1983] characterized by the minimum critical taper [Dahlen, 1984] on the pro-wedge side and the maximum critical taper on the retro-wedge side (terminology as per Willett et al. [1993]). Figure 1 illustrates two orogens with well-defined two-sided wedge geometries with steeper retro-wedges. Here we assume strict adherence to this simple critical taper wedge geometry. Further, we make the simplifying assumption that the mean topographic gradient ($\tan \alpha$ in the terminology of Davis et al. [1983]) is invariant with orogen width, tectonic influx rate, climate, and time. This implies that frictional properties, pore pressures, and the dip of the basal decollement are similarly invariant. Although we acknowledge that many factors may produce deviations from this simplest model (e.g., stratigraphic control of the basal decollement, including inherited sedimentary basin geometry and rotation in response to isostatic compensation of crustal thickening [Boyer, 1995; Lawton et

al., 1994], potential climatic and tectonic influences on basal pore pressures [Saffer and Bekins, 2002], etc.), the imposed self-similar growth of the orogenic wedge is consistent with maintenance of Airy isostatic compensation of the thickening wedge, as will be assumed here.

[5] Dahlen and colleagues demonstrated in the late 1980s and early 1990s that the erosion rate controls steady state (flux mass balance) wedge width and that deformation patterns are largely dictated by surface erosion [Dahlen, 1988, 1990; Dahlen and Barr, 1989; Dahlen and Suppe, 1988]. However, these authors employed an arguably oversimplified erosion rule, in which erosion rate was either held constant (independent of the topography) or increased linearly with elevation in a one-sided wedge with a rigid backstop. Driven in part by interest generated by these papers and by the numerical modeling efforts that followed [e.g., Avouac and Burov, 1996; Beaumont et al., 1992, 1996; Koons, 1989, 1995; Willett, 1999a; Willett et al., 1993, 2001], the last decade has seen an intense flurry of research on the processes and rates of erosion in bedrock channels. Bedrock channels have been the focus of attention because they dictate much of the relief structure of mountainous areas, communicate signals of tectonic, climatic, and eustatic change across landscapes, and ultimately set regional rates of denudation [e.g., Burbank et al., 1996; Howard et al., 1994; Whipple and Tucker, 1999]. Although many important questions remain in the study of bedrock channels and the controls on their incision rates, we are now in a position to extend the work of Dahlen and colleagues [Dahlen, 1988, 1990; Dahlen and Barr, 1989; Dahlen and Suppe, 1988] by adopting a more realistic erosion model and generalizing the treatment for application to two-sided wedges [e.g., Koons, 1990; Willett et al., 1993].

[6] The approximate analytical solution for steady state orogen width, orogen-scale strain partitioning, and rock uplift rates presented here consists of two parts. The first is essentially a statement of mass balance in an orogenic wedge at flux steady state (as per Willett and Brandon [2002]). The solution combines the geometric constraints of critical taper theory with geomorphic constraints on erosion rates consistent with this topography to find the wedge width required to satisfy the mass balance condition. We assume that erosion rates are dictated by the bedrock channel network and are described by the stream power model of bedrock channel incision [e.g., Howard and Kerby, 1983; Howard et al., 1994; Whipple and Tucker, 1999]. A similar approach has been taken by Hilley et al. [2004] and Hilley and Strecker [2004] in an analysis of one-sided frictional wedges with a fixed rooting depth for the basal detachment. Their analysis is, however, different from ours in some important details and focuses on different, complementary issues. Here we explore system sensitivity to accretionary flux, erosional efficiency (set by rock properties, channel morphology and bed state, and climate), and the first-order orographic distribution of precipitation (pro-wedge versus retro-wedge rainfall). Although the stream power model should be considered a simple, empirical, and incomplete approximation to the behavior of a complex suite of processes [e.g., Hancock et al., 1998; Sklar and Dietrich, 1998,

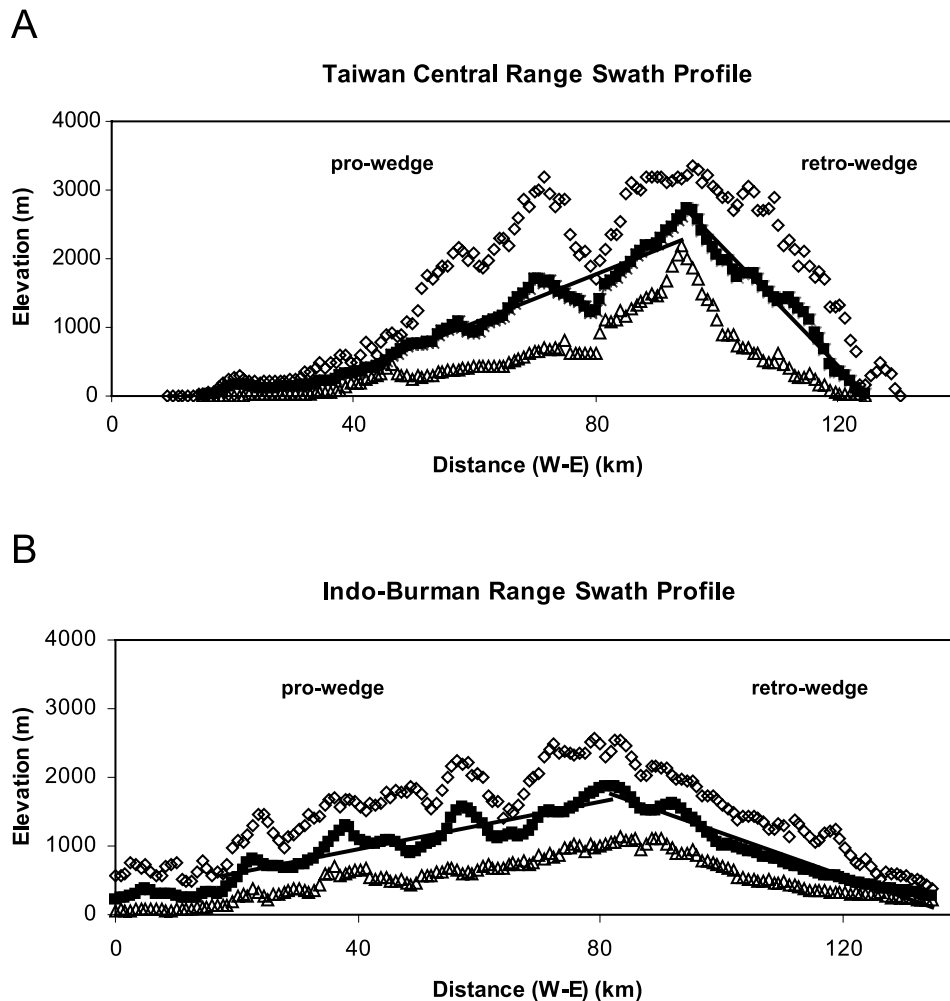


Figure 1. Example topographic cross sections of active orogens illustrating typical two-sided tapered wedge forms: (a) Central Range of Taiwan and (b) Indo-Burman Range. Plotted are maximum (diamonds), mean (squares), and minimum (triangles) elevations in ~ 50 -km-wide swath profiles taken from the GTOPO-30 30-arc-second (~ 1 km) resolution digital elevation model. Straight lines are linear regressions to the mean elevations, shown only to demonstrate the close approximation to a critical taper form.

2001; Whipple and Tucker, 2002; Whipple *et al.*, 2000], it is sufficiently general and its dynamics sufficiently well known to allow elucidation of how and why the details of the geomorphic process law matter to orogen evolution.

[7] The second part of the solution presented here is an extension of the kinematic model for time-averaged particle paths through an orogenic wedge developed by Dahlen and colleagues [Dahlen, 1988; Dahlen and Barr, 1989; Dahlen and Suppe, 1988]. Importantly, in this part of the model we can relax assumptions made in the application of the stream power incision model and thus gain additional insight into the importance of the details of the erosion rule. Batt *et al.* [2001] used a similar approach with an arbitrary, but empirically constrained, erosion function in their analysis of thermochronologic data for the Olympic Mountains in Washington State. We use this approach to highlight the potential importance of factors that may influence the relation between channel concavity

and downstream variations in erosion rate, such as the intrabasin orographic distribution of precipitation [Roe *et al.*, 2002, 2003], and downstream changes in sediment flux, amount of alluvial cover, bed material grain size [Massong and Montgomery, 2000; Sklar and Dietrich, 1998, 2001; Slingerland *et al.*, 1997; Whipple and Tucker, 2002], channel width [Montgomery and Gran, 2001; Snyder *et al.*, 2003a], and the frequency of occurrence of erosive debris flows [Stock and Dietrich, 2003].

3. Erosion and Rock Uplift

[8] At orogen scale, erosion and rock uplift are intimately linked. Consideration of a very simple orogenic system reveals the nature of this linkage and helps motivate our analysis. Imagine an orogen of constant width (W), isostatically compensated, experiencing homogeneous pure shear deformation and with a fixed accretionary influx per unit distance along strike ($F_A(\text{m}^2 \text{ yr}^{-1})$) (Figure 2).

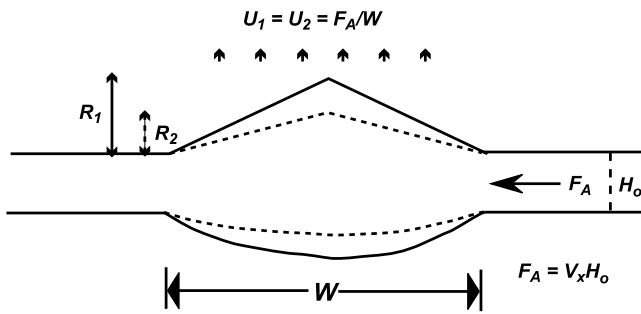


Figure 2. Cartoon illustration of a constant width orogen subjected to homogeneous pure shear deformation and maintained at Airy isostatic compensation. The steady state rock uplift rate is given by the accretionary flux divided by wedge width. In this idealized scenario, no dynamic coupling between erosional efficiency and steady state rock uplift rate is possible.

With no erosion, near-surface rock uplift rate (U) is set by isostatic compensation of crustal thickening ($U \sim ((\rho_m - \rho_c)/\rho_m)F_A/W$). With erosion that increases with topographic slope or relief, the system will evolve to a steady state where the topographic slope has increased such that erosional efflux (F_E) matches the accretionary influx (F_A). Under this condition, all accreted material is removed through the surface rather than mostly being stuffed into the crustal root, and steady state rock uplift rate increases by a factor of ~ 6 ($\rho_m/(\rho_m - \rho_c)$) to $U = F_A/W$ (Figure 2), where ρ_m and ρ_c denote mantle and crust densities as discussed by *Molnar and England* [1990], respectively. Thus rock uplift is dominantly a response to erosion. However, so long as the conditions of constant orogen width and homogeneous pure shear deformation are maintained, changes in climate-controlled erosional efficiency can influence only the form of the steady state topography, not the rock uplift rate (at steady state, $U = F_A/W$ for all climates (Figure 2)). This is the scenario implicitly considered in many analyses that impose an invariant “tectonic” uplift rate [e.g., *Whipple, 2001; Whipple et al., 1999*]. One may infer that a more interesting dynamic coupling between erosional efficiency and rock uplift rate can only occur where the intensity or spatial distribution of erosion can induce a concentration of strain, either through narrowing of the orogen or through the development of discrete shear zones that accommodate focused uplift, as seen in some coupled thermomechanical–surface process models [e.g., *Beaumont et al., 1996; Willett, 1999a*]. Critical taper theory [*Dahlen, 1984; Dahlen and Suppe, 1988; Dahlen et al., 1984; Davis et al., 1983*] provides a framework for considering how erosional efficiency may influence orogen width, rock uplift rate, and deformation within the wedge, thereby allowing an exploration of the dynamic coupling between climate-driven erosion and tectonics.

4. General Relations for Mass Balance, Steady State Wedge Geometry, and Rock Uplift Rates

[9] A closed form solution for the interrelations among steady state orogen width, rock uplift rate and pattern, and climate can be found by combining (1) a statement of mass

balance in a steady state orogenic wedge, (2) the geometry dictated by critical taper theory for a frictional wedge (e.g., Figures 1 and 3), and (3) an orogen-scale erosion rule. Here we explore a generic orogen-scale erosion rule to highlight the importance of its correct formulation.

4.1. Mass Balance

[10] A statement of mass balance for a steady state orogenic wedge (where accretionary influx balances the erosional efflux) can be written as

$$F_A = U_p W_p + U_r W_r, \quad (1)$$

where we define F_A to be the total accretionary flux per unit distance along strike ($\text{m}^2 \text{yr}^{-1}$) (including any recycled sediment eroded off pro-wedge), U_p to be the average rock uplift (or erosion) rate in pro-wedge, and U_r to be the average rock uplift (or erosion) rate in retro-wedge (m yr^{-1}) (Figure 3). W_p and W_r denote the plan view width of the pro-wedge and retro-wedge, respectively (m) (Figure 3). We define rock uplift rate (U_p, U_r) as the rate of rock uplift relative to the geoid, measured at the Earth’s surface. Note that the vertical component of rock motion is generally expected to vary with depth in a deforming orogenic wedge [e.g., *Dahlen, 1988; Dahlen and Barr, 1989*]. Rock uplift rate defined in this way is by definition equal to the erosion rate at flux steady state [*England and Molnar, 1990*]. Our discussion is cast in terms of near-surface rock uplift rate (U) (rather than erosion rate) in order to (1) emphasize the control of climate-determined and lithology-determined erosional efficiency on the deformation and uplift of rock and to (2) accommodate subsequent work on unsteady orogen evolution, where erosion rate and rock uplift rate are not equal.

[11] Equation (1) can be rewritten in a convenient form by defining λ as the fraction of the total accretionary flux that is eroded off the pro-wedge side:

$$U_p = \frac{\lambda F_A}{W_p} \quad (2a)$$

$$U_r = \frac{(1 - \lambda) F_A}{W_r}. \quad (2b)$$

[12] The total accretionary flux can then be written in terms of the incoming flux of new material (F_{A0}) by defining

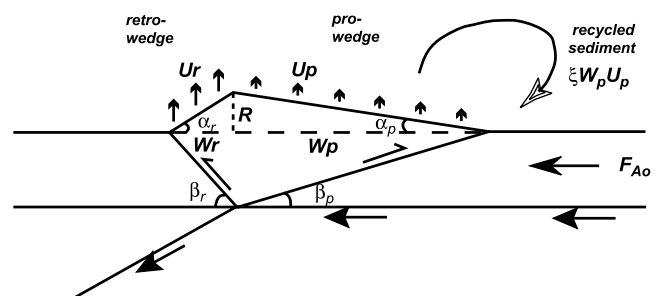


Figure 3. Definition sketch defining assumed geometry of the wedge and the major variables discussed in the text.

ξ as the fraction of material eroded off the pro-wedge that is recycled back into the orogen (Figure 3):

$$F_A = \frac{F_{A_0}}{(1 - \xi\lambda)} \quad (3a)$$

$$F_{A_0} = V_x H, \quad (3b)$$

where ξ and λ range from 0 to 1 by definition, V_x is the plate convergence velocity (m yr^{-1}), and H is the thickness of the incoming plate (including any overlying sediments) that is involved in deformation (m). One might ask how steady state can be achieved if all material eroded off the pro-wedge is recycled back into the orogen ($\xi = 1$). The answer is simply that the erosional flux off the retro-wedge (F_{Er}) must balance the far-field tectonic flux (F_{A_0}). The case of $\lambda = 1$ (zero erosion on the retro-wedge) is equivalent to the solution for a one-sided wedge with a rigid backstop, in which case a steady state solution is not possible for $\xi = 1$ (total accretionary influx grows without bound (equation (3a), precluding a steady state in this case only).

4.2. Critical Taper Geometry

[13] Given that the mean topographic relief between the range crest and foreland (R) is given by the product of wedge width (W) and the topographic taper ($\tan \alpha$), and must be the same for pro-wedge and retro-wedge (Figure 3), the geometry of the deforming wedge can be expressed as

$$\frac{W_r}{W_p} = \frac{\tan \alpha_p}{\tan \alpha_r}, \quad (4)$$

where α_p and α_r denote the taper angle of the mean topography on the pro-wedge and retro-wedge, respectively (Figure 3). For a given set of frictional properties and pore pressure conditions, α_p is dictated by the inclination of the pro-wedge basal detachment and the minimum critical taper, whereas α_r is dictated by the inclination of the retro-wedge thrust and the maximum critical taper angle [Dahlen, 1984; Willett *et al.*, 1993].

[14] As a first approximation, we assume that α_p and α_r are invariant with orogen width, accretionary flux, and climate. Obviously, this is a simplification of a complex problem, particularly in thin-skinned fold and thrust belts, where detachment surfaces are often stratigraphically controlled and thus depend on initial sedimentary basin geometry, may change during growth and widening of the wedge, and may be rotated to steeper angles as the growing wedge is isostatically compensated [e.g., Boyer, 1995; Lawton *et al.*, 1994]. Nonetheless, both the constant taper angle assumed here and the associated self-similar growth of the wedge are consistent with Airy isostatic compensation of the thickening orogenic wedge. Airy isostatic compensation is thus implicitly assumed in our analysis.

4.3. Importance of the Erosion Rule

[15] Once an erosion rule is specified, equations (2)–(4) can readily be solved for steady state orogen width and therefore rock uplift rate as a function of accretionary flux, erosional efficiency, and wedge geometry. A difficulty is

that a process-based, orogen-scale erosion rule has never been derived. This is a key goal of this paper, addressed in section 5. We begin here with a very general erosion rule to illustrate how and why the form of the erosion rule is important and to place our analysis into context with previous work.

[16] One may infer that the orogen-scale average erosion rate (E (m yr^{-1})) must depend (at least) on both orogen width and the mean topographic gradient. We posit a simple power law form for our general erosion law:

$$E = CW^a (\tan \alpha)^b, \quad (5)$$

where C is a dimensional coefficient of erosional efficiency ($\text{m}^{1-a} \text{yr}^{-1}$) (set by climate, rock properties, and channel characteristics) and a and b are positive constants set by the physics of erosion and the network geometry and relief structure of drainage basins. Note that previous analytical work on this problem either assumed a constant erosion rate with no relation to the topography ($a = b = 0$) or a relation in which mean erosion rate scaled with mean elevation or equivalently total relief ($a = b = 1$) [see Dahlen and Barr, 1989; Dahlen and Suppe, 1988, and references therein]. These previous efforts were further limited to a one-sided wedge with no recycling of material ($\lambda = 1$; $\xi = 0$).

[17] At flux steady state, $E = U$ by definition, and equation (5) may be substituted into equation (2a) to solve for steady state pro-wedge width (W_p):

$$W_p = \left(\frac{\lambda F_A}{C_p} \right)^{\frac{1}{a+1}} (\tan \alpha_p)^{\frac{b}{a+1}}, \quad (6)$$

where C_p is the erosional efficiency on the pro-wedge. Substituting equation (6) back into equation (2a), we can also readily solve for the steady state pro-wedge rock uplift rate (U_p):

$$U_p = (\lambda F_A)^{\frac{a}{a+1}} C_p^{\frac{1}{a+1}} (\tan \alpha_p)^{\frac{b}{a+1}}. \quad (7)$$

Solutions for the retro-wedge differ only in that W_p , U_p , C_p , $\tan \alpha_p$, and λ are replaced by W_r , U_r , C_r , $\tan \alpha_r$, and $1 - \lambda$, respectively. Recall that F_A is the total accretionary flux, including any recycled sediment, as defined in equation (3).

[18] Several conclusions can be drawn immediately. First, for all exponent values, steady state wedge width is equally sensitive to accretionary flux (F_A) and the inverse of erosional efficiency (C^{-1}). This sensitivity is set by the relation between mean erosion rate and wedge width (exponent a). Second, the relative sensitivity of steady state rock uplift rate to accretionary flux and erosional efficiency also depends on the exponent a : Rock uplift rate is more sensitive to erosional efficiency for $a < 1$ and more sensitive to accretionary flux for $a > 1$. Third, in the case $a = 0$ considered in many previous works [e.g., Barr and Dahlen, 1989; Dahlen, 1988, 1990], rock uplift rate is linearly dependent on the erosional efficiency and independent of accretionary flux. In contrast, the $a = 1$ case considered by Dahlen and Suppe [1988] and Dahlen and Barr [1989], rock uplift rate is set by the square root of the ratio of accretionary flux to erosional efficiency. Thus Dahlen and

Barr's [1989, p. 3911] conclusion that the form of the erosion law is not important is incorrect and stems from their limited analysis of this aspect of the problem.

[19] In the above the dependence of erosion rate on mean topographic gradient does not appear, at first glance, to play an important role. It does, however, importantly influence the relative rate of erosion on the pro-wedge and retro-wedge sides of the orogen, which in turn sets λ , the fraction of material eroded off the pro-wedge. This can be seen by writing the ratio of E_p/E_r (denoted below as ϕ) using equation (5), assuming a and b are the same on the pro-wedge and retro-wedge and noting that at flux steady state, $E_p/E_r = U_p/U_r$ by definition:

$$\phi = \frac{U_p}{U_r} = \frac{C_p}{C_r} \left(\frac{\tan \alpha_p}{\tan \alpha_r} \right)^{b-a}. \quad (8)$$

Note that the C_p/C_r ratio reflects not only climatic but also lithologic differences between the pro-wedge and retro-wedge. Combining equation (8) with the mass balance constraint yields an expression for the fraction of total accretionary flux that is eroded off the pro-wedge (λ). This is found by taking the ratio of equations (2a) and (2b), substituting ϕ for the U_p/U_r ratio (as defined in equation (8)), and solving for λ using equation (4):

$$\lambda = \frac{\phi}{(\tan \alpha_p / \tan \alpha_r) + \phi}. \quad (9)$$

[20] Since $\tan \alpha_r > \tan \alpha_p$ [Dahlen, 1984], for uniform erosional efficiency ($C_p/C_r = 1$), erosion rates (and rock uplift rates) will be equal on the pro-wedge and retro-wedge sides of the orogen if and only if $a = b$ (i.e., for a simple power law relation between mean elevation (or total relief) and erosion rate). Other combinations of a and b will importantly influence λ , a measure of strain partitioning between the pro-wedge and retro-wedge. In addition to its role in equations (6) and (7), it will be shown later that for frontal accretion without underplating, λ largely dictates particle trajectories through the orogen and thus exerts a fundamental control on particle pressure-temperature-time paths and the spatial distribution of both the metamorphic grade of exposed rocks and thermochronologic ages [e.g., Barr and Dahlen, 1989; Barr et al., 1991; Batt and Brandon, 2002; Batt et al., 2001; Dahlen and Barr, 1989; Dahlen and Suppe, 1988; Koons, 1987; Willett and Brandon, 2002]. Thus it is clear that the form of the erosion law plays a critical role in the interaction between surface processes and geodynamic evolution of a two-sided orogenic wedge. The relations among model parameters (C , a , b), the processes of erosion, and environmental conditions (climate, lithology) therefore stand out as important unknowns.

5. An Orogen-Scale Erosion Rule

[21] In order to derive a physically based orogen-scale erosion rule, we start by considering the steady state relationship between erosion rate (or rock uplift rate) and topography. We write relations for steady state topography in terms of the simple detachment-limited stream power

river incision model [Howard et al., 1994; Whipple and Tucker, 1999]. The stream power incision model can be considered a placeholder for more sophisticated models as advances are made. However, it is important to note that the solution developed here rests on three core assumptions and beyond these is not strongly tied to the stream power incision model and its potential limitations. The three fundamental assumptions are that (1) equilibrium river profiles maintain a form captured by the commonly seen power law relation

$$S = k_s A^{-\theta}, \quad (10)$$

where S is local channel gradient, A is upstream drainage area (m^2), k_s is the steepness index (positive) ($m^{2\theta}$), and θ is the concavity index; (2) there is a power law relationship between the steepness index and both rock uplift rate and erosional efficiency; and (3) the concavity index (θ) is invariant with both rock uplift rate and erosional efficiency. The first is strongly supported empirically [e.g., Flint, 1974; Kirby and Whipple, 2001; Kirby et al., 2003; Sklar and Dietrich, 1998; Snyder et al., 2000; Tarboton et al., 1989; Tucker and Whipple, 2002] and appears to hold for both detachment-limited and transport-limited conditions, even in some (but not all) systems that appear to be far from equilibrium [Whipple and Tucker, 2002; Willgoose, 1994]. The second and third requirements are more controversial and therefore most limiting [Sklar and Dietrich, 1998, 2001; Stock and Dietrich, 2003], but as shown in Figure 4, they are also well supported where field constraints allow direct testing of the hypothesis that these assumptions are valid [Kirby and Whipple, 2001; Kirby et al., 2003; Snyder et al., 2000, 2003b; Wobus et al., 2003].

[22] The detachment-limited stream power model satisfies all three conditions (as do standard transport-limited models and certain hybrid models [see, e.g., Whipple and Tucker, 2002]). Even where assumptions 2 and 3 appear robust, however, several incompletely understood factors influence the quantitative relationships among channel steepness, rock uplift rate, and climate, including dynamic adjustments in channel width [Montgomery et al., 2002; Snyder et al., 2003a], sediment flux, percent alluvial bed cover, bed load grain size distribution [Hancock and Anderson, 2002; Massong and Montgomery, 2000; Sklar and Dietrich, 1998, 2001; Whipple and Tucker, 2002], channel hydraulic roughness, the relative importance of a critical shear stress for incision [Snyder et al., 2003b; Tucker, 2004], the relative importance of debris flow scour [Stock and Dietrich, 2003], and orographic precipitation feedbacks [Roe et al., 2002, 2003]. Although we do not tackle these problems here, our analysis will show how important these factors, through their influence on the rates and patterns of bedrock channel incision, can be in orogen evolution. Thus the detachment-limited stream power incision model is sufficiently robust and general for our present purposes.

5.1. Steady State Fluvial Relief

[23] Given the three assumptions stated above, fluvial relief (R_f) is given by integrating equation (10), using Hack's law ($A = k_a x^h$) [Hack, 1957], from the basin outlet

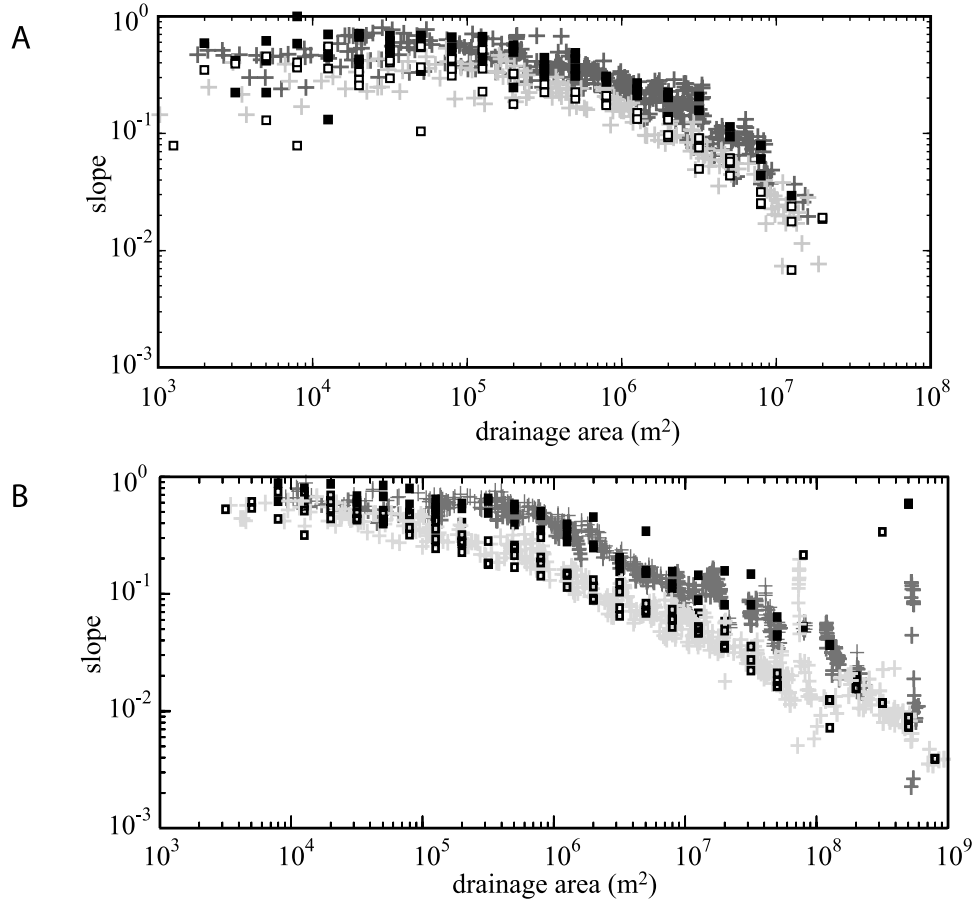


Figure 4. Example slope-area relationships for two field areas with known spatial patterns in rock uplift rate. (a) King Range, Mendocino Triple Junction region, northern California [Merritts and Bull, 1989; Snyder *et al.*, 2000]. (b) San Gabriel Mountains, southern California [Blythe *et al.*, 2000]. These data illustrate the typical scaling relation between channel gradient (“slope”) and upstream drainage area (equation (10)). Importantly, in both field settings the steepness index (k_s) alone varies with rock uplift rate; the low-uplift (gray crosses and open squares for log-bin average values) and high-uplift zone (black crosses and solid squares for log-bin average values) slope-area arrays are subparallel in both cases.

($x = L$) to the fluvial channel head ($x = x_c$), as shown by Whipple and Tucker [1999]:

$$R_f = k_s k_a^{-\theta} (1 - h\theta)^{-1} (L^{1-h\theta} - x_c^{1-h\theta}). \quad (11)$$

Note that k_a is a dimensional coefficient (m^{2-h}). In the particular case of the detachment-limited stream power model at steady state,

$$E = U = KA^m S^n, \quad (12)$$

where E is erosion rate (myr^{-1}), K is a dimensional coefficient of fluvial incision ($\text{m}^{1-2m} \text{yr}^{-1}$), and channel steepness and concavity indices are given by $k_s = (U/K)^{1/n}$ and $\theta = m/n$, respectively. We substitute these definitions for k_s and θ for the stream power model at steady state into equation (11) to write fluvial relief as [Whipple and Tucker, 1999]

$$R_f = U^{1/n} K^{-1/n} k_a^{-m/n} (1 - hm/n)^{-1} (L^{1-hm/n} - x_c^{1-hm/n}). \quad (13)$$

[24] The difference term involving x_c in equation (13) is awkward for the derivation below. For orogen-scale drain-

ages like those of interest here, L is on the order of 20–200 km and x_c is on the order of 0.1–1 km, suggesting that the assumption $L \gg x_c$ may be made. However, the exponent $(1 - hm/n)$ is typically around 0.15 ± 0.1 , and while $L^{1-hm/n} > x_c^{1-hm/n}$, dropping the x_c term can be somewhat problematic for certain combinations of model parameters (low values of $1 - hm/n$), though as we will see does not, in fact, much affect our analysis. Nonetheless, we can deal with this difficulty through a dimensionless correction factor (k_0), defined by

$$R_f = U^{1/n} K^{-1/n} k_a^{-m/n} (1 - hm/n)^{-1} (L^{1-hm/n}) k_0 \quad (14a)$$

$$k_0 = 1 - (x_c/L)^{1-hm/n}, \quad (14b)$$

where k_0 may be expected to be of order unity but varies with L , x_c , and the exponent $1 - hm/n$, unless the approximation $L^{1-hm/n} \gg x_c^{1-hm/n}$ holds. For $L \gg x_c$ the relation between k_0 and L can be approximated as a power law, which is convenient for our analysis. We turn to regression analysis to evaluate the robustness of a power

law approximation and find it valid, provided $(x_c/L)^{1-hm/n}$ is less than ~ 0.6 or for $L > 20$ km (the smallest system size of interest here), given the typical range of x_c (0.1–1 km) and the hm/n ratio (0.85 ± 0.1).

[25] The correction factor, k_0 , varies from 0.4 to 0.85 (low k_0 values correspond to low values of exponent $1 - hm/n$) and is a power law function of channel length (L):

$$k_0 = k_* L^q, \quad (15)$$

where k_* is a dimensional coefficient (m^{-q}) and $R^2 > 0.99$ for all reasonable values of h , m/n , and x_c . Both k_* and q vary slightly with x_c and the exponent $1 - hm/n$. Computing k_* and q values for a reasonable range of x_c and the exponent $1 - hm/n$ and regressing the results for a typical x_c (0.5 km) against $1 - hm/n$, we find the following relations:

$$q = 0.20 - 0.32(1 - hm/n), \quad R^2 = 0.998, \quad (16a)$$

$$k_* = 1.38(1 - hm/n)^{0.85}, \quad R^2 = 0.999. \quad (16b)$$

[26] In equation (16a) the coefficient is invariant with x_c in the range 0.1–1 km, and the constant varies only by ± 0.03 . In equation (16b) the coefficient and exponent each vary only by ± 0.06 with x_c over this same range. Thus for the typical range of h , m/n , and x_c , regression parameters in equation (15) vary only slightly around their mean values ($q = 0.12 \pm 0.03$ with either x_c or $1 - hm/n$; $k_* = 0.42 \pm 0.12$ with $1 - hm/n$ and 0.42 ± 0.06 with x_c). Therefore the convenient approximation in equation (14a) is reasonably accurate, with $k^* = 0.4$ and $q = 0.1$ in equation (15). Greater precision can be achieved by using the relations in equation (16), as is done below. Making the simple assumption that $L^{1-hm/n} \gg x_c^{1-hm/n}$ would be equivalent to assuming $k^* = 1$ and $q = 0$.

[27] In order to proceed, we must relate channel length (L) to orogen half width (W). Studies of drainage network structure have generally found the relation between channel length and axis-parallel basin length (equivalent to the orogen half width, W , for the major transverse drainage basins with their headwaters at the divide) is approximately linear, with a proportionality constant of order unity [Maritan *et al.*, 1996; Rigon *et al.*, 1996; Tarboton *et al.*, 1988, 1989]. This finding is also clearly illustrated by the fact that whereas the reciprocal of the Hack exponent (h) is always close to but just less than 2 [Maritan *et al.*, 1996; Rigon *et al.*, 1996; Tarboton *et al.*, 1988, 1989], Montgomery and Dietrich [1992] found that basin area was related to the square of axis-parallel basin length over many orders of magnitude. These results are only mutually compatible if there is an approximately linear relation between L and W , which we assume here:

$$L = k_1 W, \quad (17)$$

where k_1 is a dimensionless coefficient of order unity. Any deviation from the linear relation assumed in equation (17) is minor and will not significantly influence our analysis.

[28] Finally, using equations (14), (15), and (17), fluvial relief on pro-wedge and retro-wedge sides of orogen can be written as

$$R_p = U_p^{1/n} K_p^{-1/n} \chi W_p^{1-hm/n+q}, \quad (18)$$

$$R_r = U_r^{1/n} K_r^{-1/n} \chi W_r^{1-hm/n+q}, \quad (19)$$

$$\chi = k_* k_1^{1-hm/n+q} k_a^{-m/n} (1 - hm/n)^{-1}, \quad (20)$$

where K_p and K_r denote the coefficient of erosion (reflecting both climatic and lithologic differences) on the pro-wedge and retro-wedge, respectively, and we have assumed that (1) U is approximately constant on either side of the wedge and that (2) k^* , k_1 , k_a , h , m , and n are the same on the pro-wedge and retro-wedge such that χ is a (dimensional) constant ($m^{hm/n-2m/n-q}$). Close agreement in k^* , k_1 , k_a , and h on either side of the orogen is expected, so this assumption is not particularly restrictive. The assumption that the effective values of m and n are the same on both sides is more restrictive as notable differences in these parameters with climate state, rock type, critical shear stress, and sediment flux and caliber are certainly plausible [Hancock *et al.*, 1998; Sklar and Dietrich, 1998, 2001; Snyder *et al.*, 2003b; Whipple and Tucker, 2002; Whipple *et al.*, 2000; Whipple and Tucker, 1999]. Although no specific evidence that this is indeed the case in any orogen has yet been published, holding m and n equal on either side of the range and invariant with climate, lithology, and rock uplift rate must be regarded as a simplifying assumption necessary to make an analytical solution tractable. The assumption that U_p and U_r are approximately constant (but not necessarily equal) will be relaxed later in the kinematic solution for particle trajectories through the wedge, allowing us to explore just how sensitive orogen evolution is to the details of the erosion process law.

5.2. Channel Profiles and the Mean Topographic Gradient

[29] Further progress requires defining the quantitative relationship between the gradients, drainage areas, and spatial distribution of bedrock channels driving the erosion (as represented in equations (18) and (19)) and the regional gradient of the mean topography ($\tan \alpha$) that is set by the mechanics of the deforming wedge. If this can be achieved, predictions of steady state orogen width, relief, rock uplift rates, crustal thickness, and their sensitivity to variables like the accretionary flux and erosional efficiency can be made, thus elucidating the salient characteristics of the dynamic coupling between climate-driven erosion and tectonics.

[30] Incision occurs on bedrock channel floors throughout the channel network and is driven by flow discharge, sediment flux and grain size, and channel gradient [e.g., Howard and Kerby, 1983; Howard *et al.*, 1994; Sklar and Dietrich, 1998, 2001; Whipple and Tucker, 1999, 2002]. However, it is the mean topography that is relevant to the geodynamics of the orogen. This difference in scale is a problem hidden in most coupled tectonic and surface process models of actively eroding orogens. One cannot

simply apply rules developed for bedrock channels to a mean topographic profile without defining the relation between channel longitudinal profiles and the mean topographic gradient. Although this appears to be a dauntingly complex problem involving the full richness of drainage network topology and controls on hillslope length and gradient to define a “relief function” that relates a channel profile to ridgelines and the regional mean topographic gradient, we present a simple, empirically supported, approximate relationship between them.

[31] As stated earlier, the mean elevation of the divide (above the foreland) of a two-sided orogenic wedge is, by definition, given by the product of wedge half width (e.g., W_p) and the critical topographic taper (e.g., $\tan \alpha_p$). Given that (1) the fluvial relief (R_f) of major drainage basins that rise on the divide must scale with the mean elevation of the range crest and that (2) trunk channel length scales approximately linearly with wedge half width (equation (17)), inspection suggests that the ratio of fluvial relief to trunk channel length scales approximately linearly with the mean topographic gradient. Although this step may seem an oversimplification, the expected relation is empirically observed to be linear with a dimensionless prefactor (k_2 in equation (21a)) of order unity (Figure 5):

$$\frac{R_f}{L} = k_2 \tan \alpha \quad (21a)$$

$$\frac{R_f}{W} = k_1 k_2 \tan \alpha. \quad (21b)$$

Figure 5a shows a test of this hypothesis using a composite of data from natural examples (Central Range of Taiwan and the Indo-Burman Range, shown in Figure 1) and from synthetic steady state landscapes computed using the Geomorphic/Orogenic Landscape Evolution Model (described by *Tucker and Slingerland* [1996]). The result is quite satisfying: There is an approximate 1:1 relationship between R_f/L and $\tan \alpha$ (i.e., equation (21a) holds with $k_2 \sim 1$). Although some complexity is evident (Figure 5a) and will be discussed in section 8.6, equation (21) appears sufficiently robust to proceed.

5.3. Derivation of the Erosion Rule

[32] The approximate relation above (equation (21b)) allows us to write the erosion rule of equation (12) in terms of orogen width (W) and regional topographic gradient ($\tan \alpha$). The key is to find the relationship between steady state channel gradient at the mountain front (S_L) and $\tan \alpha$. This is done by solving equation (12) for S_L , using Hack’s law to write the main stem drainage area at the mountain front in terms of channel length (L), substituting in the solution for steady state fluvial relief (equation (18) or (19)), and, finally, substituting equation (21b) into this expression for steady state channel gradient at the mountain front:

$$S_L = k_*^{-1} k_1^{-q} k_2 (1 - hm/n) W^{-q} \tan \alpha. \quad (22)$$

Using Hack’s law and equation (17) to write main stem drainage area at the mountain front in terms of orogen width

(W) ($A = k_a k_1^h W^h$) and substituting this expression and equation (22) into equation (12) gives

$$E = U = K' W^{hm-qn} (\tan \alpha)^n \quad (23a)$$

$$K' = K k_*^{-n} k_1^{hm-qn} k_2^n k_a^m (1 - hm/n)^n, \quad (23b)$$

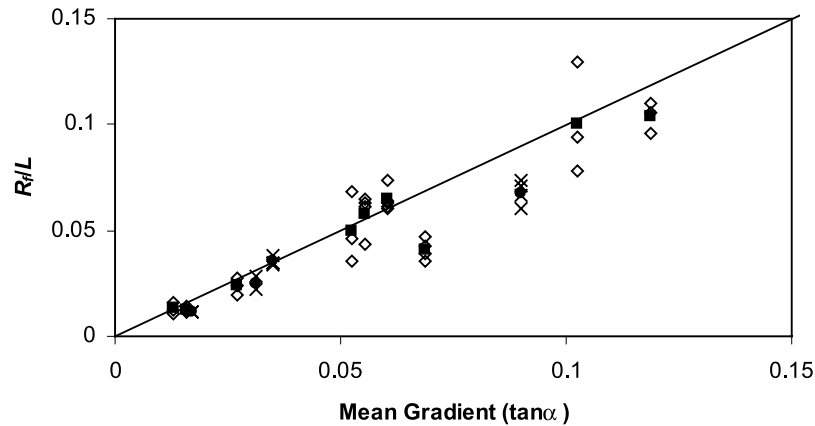
which holds for either side of the wedge (e.g., with U_p , W_p , $\tan \alpha_p$, and K_p for the pro-wedge). Equation (23a) is equivalent to the general erosion law introduced earlier (equation (5)), with $C = K'$, $a = hm - qn$, and $b = n$. Note that K' is a dimensional coefficient ($m^{1-hm+qn} \text{ yr}^{-1}$) that is linearly related to the coefficient of fluvial incision (K). Note that this expression is derived directly from the river incision rule of equation (12) using only the geometric approximations in Hack’s law, equation (17), and equation (21b) and no other considerations related to the mechanics of a brittle wedge or the formulation of the tectonic problem addressed in this paper.

[33] Although equations (23a) and (23b) look complex, we emphasize that k_* , k_1 , k_2 , k_a , h , q , and the ratio m/n are essentially geometric constants with a fixed, narrow range of values: ~ 0.4 , ~ 1 , ~ 1 , ~ 6.7 , ~ 1.67 , ~ 0.1 , and ~ 0.5 , respectively. These parameters are included here mostly for completeness; system behavior depends primarily on the parameters in the stream power incision model (K , m , and n in equation (12)). However, in practice, it is critical to remember that K' , K , k_* , and k_a are dimensional constants with dimensions that depend on model parameters m , n , h , and q : One can not freely vary these model exponents while holding K' , K , k_* , and k_a at fixed values and expect to get reasonable predictions of orogen width, rock uplift rate, and so forth. Careful tracking of dimensions and application of the internal relations among various interdependent model parameters is critical. See *Whipple and Tucker* [1999] for a complete derivation of the coefficient of fluvial incision (K), including internal relations that determine its dimensionality. As discussed elsewhere [*Hancock et al.*, 1998; *Whipple et al.*, 2000; *Whipple and Tucker*, 1999], model exponents m and n depend on the physics of fluvial incision into rock, with the slope exponent (n) plausibly ranging from 2/3 to 5/3, depending on the dominant incision process. In addition, internal feedbacks in the river incision process not explicitly treated in the stream power model (such as adjustments in channel width, bed state, orographic enhancement of precipitation, and the relative importance of a critical shear stress for incision) may be manifest as higher effective values of n [e.g., *Snyder et al.*, 2000, 2003a, 2003b; *Tucker*, 2004] as these can importantly influence the quantitative relationship between channel steepness and rock uplift rate ($k_s = (U/K)^{1/n}$ for the detachment-limited stream power incision model).

6. Implications for Feedback Between Climate-Driven Erosion and Tectonics

[34] From the preceding analysis we see that the relationship among steady state pro-wedge width, accretionary flux, and erosion model parameters can be found by

A



B

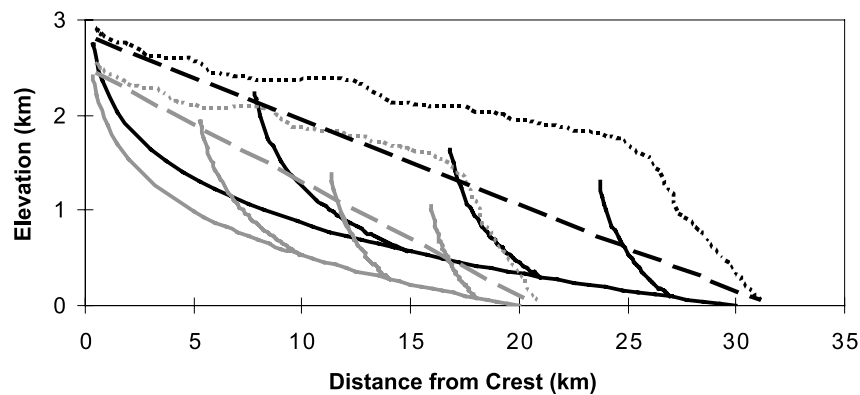


Figure 5. Relationships among channel profiles, the regional mean topographic gradient, and relative erosion rates. (a) Relationship between R_r/L and the regional mean topographic gradient from a combination of natural landscapes (pro-wedge and retro-wedge slopes of the Taiwan Central Range and Indo-Burman Range from Figure 1 are shown with crosses; solid circles are the mean of three to four measurements in the largest drainage basins) and modeled landscapes (Geomorphic/Orogenic Landscape Evolution Model) (open diamonds; solid squares are the mean of three to four measurements in the largest drainage basins). The line of 1:1 correspondence is shown (solid). Two examples (one modeled and the retro-slope of the Taiwan Central Range) fall below the 1:1 line and are examples with relief so extreme that hillslopes and colluvial channels account for a significant proportion of the total relief. (b) Relationship between the mean topographic gradient and trunk channel length (L) for steady state channel profiles eroding at the same rate. Larger basins have greater drainage areas and thus can erode faster at the same regional mean topographic gradient.

substituting $C = K'$, $a = hm - qn$, and $b = n$ into equation (6):

$$W_p = (\tan \alpha_p)^{\frac{-n}{hm-qn+1}} (\lambda F_A)^{\frac{1}{hm-qn+1}} K_p^{\frac{-1}{hm-qn+1}}, \quad (24)$$

where F_A is the total accretionary flux, including any recycled sediment (see equation (3)). Similarly, the relationship among steady state pro-wedge rock uplift rate, accretionary flux, and erosion model parameters can be found by substituting $C = K'$, $a = hm - qn$, and $b = n$ into equation (7):

$$U_p = (\tan \alpha_p)^{\frac{n}{hm+1-qn}} (\lambda F_A)^{\frac{hm-qn}{hm-qn+1}} K_p^{\frac{1}{hm-qn+1}}. \quad (25)$$

As noted earlier, solutions for the retro-wedge differ only in that W_p , U_p , K_p' , $\tan \alpha_p$, and λ are replaced by W_r , U_r , K_r' , $\tan \alpha_r$, and $1 - \lambda$, respectively.

[35] Figures 6a and 6b illustrate how the relations for mass balance and the orogen-scale erosion rule together dictate steady state wedge width and rock uplift rate (illustrated for the pro-wedge only, assuming $K_r = K_p$). The nature of the dynamic coupling between erosional efficiency and rock uplift rate is illustrated in Figure 6a, and that between accretionary flux and rock uplift is illustrated in Figure 6b. An increase in erosional efficiency induces a significant increase in rock uplift rate, damping the sensitivity of landscape relief to climate change [Whipple *et al.*, 1999]. Controls on exponent values and implications of equations (24) and (25) are discussed in sections 6.1 and 6.2.

[36] We are also now in a position to evaluate the controls on relative rock uplift rates on either side of the orogen.

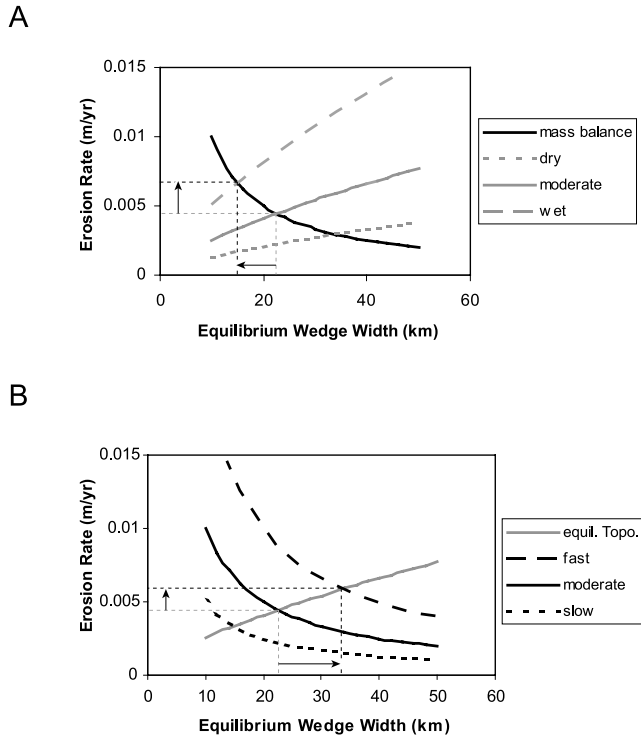


Figure 6. Illustration of how relations for mass balance and orogen-scale erosion rate combine to define the steady state wedge width (and therefore relief) and rock uplift (or, equivalently, erosion) rate (intersection of curves indicates the steady state solution; see thin dashed lines). (a) Illustration of how steady state wedge width and steady state rock uplift rate respond to differences in erosional efficiency (here qualitatively labeled as “wet” and “dry” for high and low erosional efficiencies, respectively). Arrows emphasize the narrowing and acceleration of rock uplift accompanying a transition from “moderate” to “wet” conditions. (b) Illustration of how both wedge width and steady state rock uplift rate respond to differences in accretionary flux (here labeled as “fast” versus “slow” tectonic convergence rates). Arrows emphasize the combined widening and acceleration of rock uplift accompanying a transition from “moderate” to “fast” convergence rate.

Noting that $C_p/C_r = K_p/K_r$ and substituting $a = hm - qn$ and $b = n$ into equation (8), we find that

$$\phi = \frac{U_p}{U_r} = \frac{K_p}{K_r} \left(\frac{\tan \alpha_p}{\tan \alpha_r} \right)^{n-hm+qn}. \quad (26)$$

Equation (26) can also be found by taking the ratio of equations (18) and (19) and noting that $R_p \sim R_r$ is required by geometry. Thus the geometric constraints of a two-sided orogenic wedge at critical taper and the orographic distribution of precipitation (represented by differences in the coefficient of fluvial erosion (K) on either side of the wedge) together dictate the relative rock uplift rates on the pro-wedge and retro-wedge sides of the orogen, and therefore the partitioning of mass flux through the pro-wedge and retro-wedge (λ , equation (9)), in a simple,

predictable manner. The implications of this relation for the relative strength of the coupling among steady state orogen width, rock uplift rate, and orographically and lithologically controlled erosional efficiency on both the pro-wedge and retro-wedge sides of the orogen will be discussed in the section on nonuniform erosional efficiency (section 6.2).

6.1. Uniform Erosional Efficiency

[37] Where the coefficient of erosion is equal on both sides of the wedge ($K_p = K_r$), the dynamics of the wedge can be fully described using the relations for the pro-wedge only (equations (24) and (25)) because the partitioning of strain between the pro-wedge and retro-wedge is set by wedge geometry ($\tan \alpha_p$, $\tan \alpha_r$) and the exponents in the bedrock channel incision model alone (h , m , and n in equation (12)), as seen in equations (26) and (9). Further, because λ is fixed in this scenario, the degree to which material eroded off the pro-wedge is recycled back into the orogen (ξ in equations (3), (24), and (25)) only has the effect of changing the total accretionary flux and does not influence system response to changes in either climate or the far-field tectonic influx.

[38] The implications of the analysis above for the dynamic coupling between climate and tectonics are illustrated in Figures 7–9 and can be distilled by substituting typical ranges of model exponents h (1.6–1.8), m (.3–1), n (.67–2), and q (0.11–0.20) (reported, for instance, by *Hack* [1957], *Hancock et al.* [1998], *Tucker and Whipple* [2002], *Whipple et al.* [2000], and *Whipple and Tucker* [1999]):

$$W \propto R \propto K^{-(0.4-0.7)} F_A^{0.4-0.7} \quad (27a)$$

$$U \propto K^{0.4-0.7} F_A^{0.3-0.6}. \quad (27b)$$

Thus where $K_p = K_r$, orogen width and topographic relief are equally dependent on the inverse of erosional efficiency ($1/K$) and the tectonic accretionary flux (F_A) (Figures 7a and 8a). Rock uplift rate, however, is actually more sensitive to erosional efficiency than to accretionary flux for most values of the erosion law exponents h , m , and n (Figures 7b and 8b). Recall from equation (7) that steady state rock uplift is more strongly controlled by erosional efficiency than by accretionary flux whenever $a < 1$ or $hm - qn < 1$. Given typical values of h (~ 1.7) and m/n (~ 0.5) and the relation between q and hm/n (equation (16a)), the condition $a < 1$ is equivalent to $n < 1.4$, which, as noted in section 5.3, includes most of the expected range of this parameter [e.g., *Whipple et al.*, 2000]. However, as noted in section 5.3, internal feedbacks among topography, incision rate, and the efficiency of incision may be manifest as higher effective values of n . As such, the effect of these internal feedbacks, where present, will be to decrease the sensitivity of steady state orogen width to the F_A/K ratio (equation (24)) and to enhance the relative dependence of rock uplift rate on accretionary flux (equation (25)).

[39] For reasonable parameter values, erosion rate (and therefore steady state rock uplift rate) is predicted to be higher on the steeper retro-wedge under conditions of uniform erosional efficiency ($K_p = K_r$). Recall from equation (8) that this holds if $b > a$ or $n > hm - qn$, which, using equation (16a), can be shown to reduce to $m/n \leq 0.8$. The m/n ratio for fluvial erosion processes is predicted to

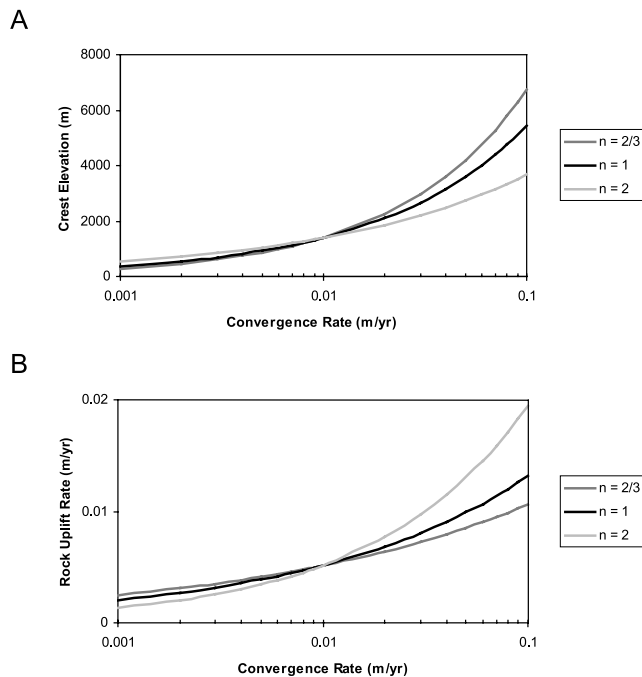


Figure 7. (a) Crest elevation (or, equivalently, topographic relief or wedge width) as a function of accretionary flux (plotted as convergence rate for a constant thickness of incoming material) for different values of the slope exponent (n) from the stream power river incision model. (b) Steady state rock uplift (or, equivalently, erosion) rate as a function of accretionary flux (plotted as convergence rate for a constant thickness of incoming material) for different values of the slope exponent (n) from the stream power river incision model.

be ~ 0.5 [Whipple and Tucker, 1999], so the finding that higher erosion and rock uplift rates are expected on the retro-wedge under uniform climatic and lithologic conditions is quite robust.

[40] It is clear that an increase in erosional efficiency (increasing K) must induce a reduction in steady state crest elevation and fluvial relief (Figure 8), although the associated dynamic increase in rock uplift damps this effect compared to expectations under the assumption that rock uplift rate is an independent, externally forced variable [see Whipple *et al.*, 1999]. The relief of active orogenic wedges at critical taper cannot be increased by uniform increases in erosional efficiency (Figure 8). This result carries an important implication for global relations between erosion rate and topographic relief [e.g., Ahnert, 1970; Montgomery and Brandon, 2002; Pazzaglia and Brandon, 1996]: Whereas data from a suite of otherwise similar steady state orogens with different accretionary influx rates would exhibit the expected positive correlation between erosion rate and relief (Figure 9a), data from a suite of otherwise similar steady state orogens in different climate zones (or with different rock erodibilities) would exhibit an inverse relation between erosion rate (or rock uplift rate) and relief (Figure 9b).

6.2. Nonuniform Erosional Efficiency

[41] System response to nonuniform changes in erosional efficiency ($K_p \neq K_r$) is more complex because the partition-

ing of strain and exhumation (represented by λ , the fraction of the accretionary flux eroded off the pro-wedge) between the pro-wedge and retro-wedge is strongly influenced by the K_p/K_r ratio (equations (26) and (9)). Consequently, steady state orogen width and rock uplift rates (U_p , U_r) show different sensitivities to changes in erosional efficiency on the pro-wedge and retro-wedge sides of the orogen. In addition, the sensitivity of the system to changes in erosional efficiency (K_p or K_r) is importantly modulated by ξ , the proportion of material eroded off the pro-wedge that is recycled into the orogen and contributes to the total accretionary flux (F_A): For $\xi \neq 0$, any change in λ directly influences the mass flux through the orogen (equations (3a), (24), and (25)). Note that λ is most sensitive for changes in either K_p or K_r when $K_p/K_r < 1$ (Figure 10).

[42] We can explore system sensitivity to the K_p/K_r ratio and the recycling of material eroded off the pro-wedge (ξ) by examining the limiting cases of complete recycling ($\xi = 1$) and no recycling ($\xi = 0$) and comparing these to the case of uniform erosional efficiency (equations (24)–(27)). We may anticipate that the change in the influence of K_p relative to the uniform erosional efficiency scenario discussed in section 6.1 will be most exaggerated by the limiting case with complete recycling. For $\xi = 1$, equations (24) and (25) can be reduced to write U_p , U_r , W_p , and W_r as power functions of both K_p and K_r because $\lambda \propto 1 - \lambda$ in equation (3a)

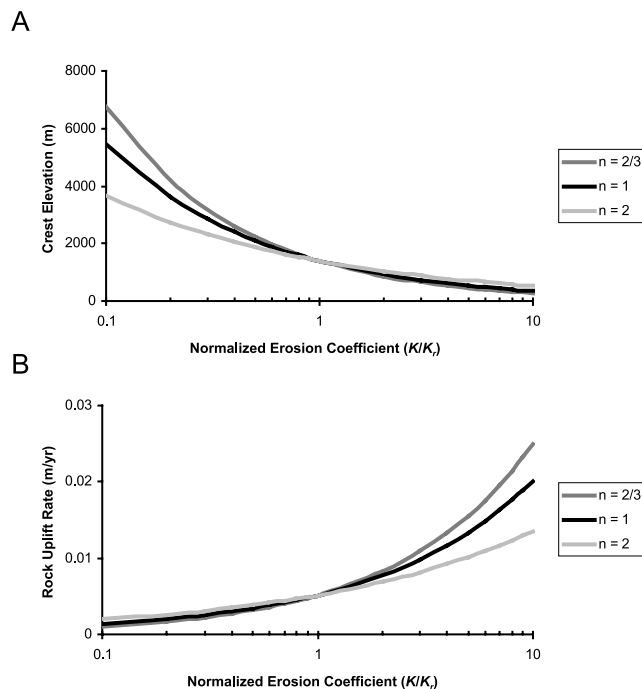


Figure 8. (a) Crest elevation (or, equivalently, topographic relief or wedge width) as a function of erosional efficiency (normalized to a reference value of K , not to the K for the retro-wedge) for different values of the slope exponent (n) from the stream power river incision model. (b) Steady state rock uplift (or, equivalently, erosion) rate as a function of erosional efficiency (normalized to a reference value of K , not to the K for the retro-wedge) for different values of the slope exponent (n) from the stream power river incision model.

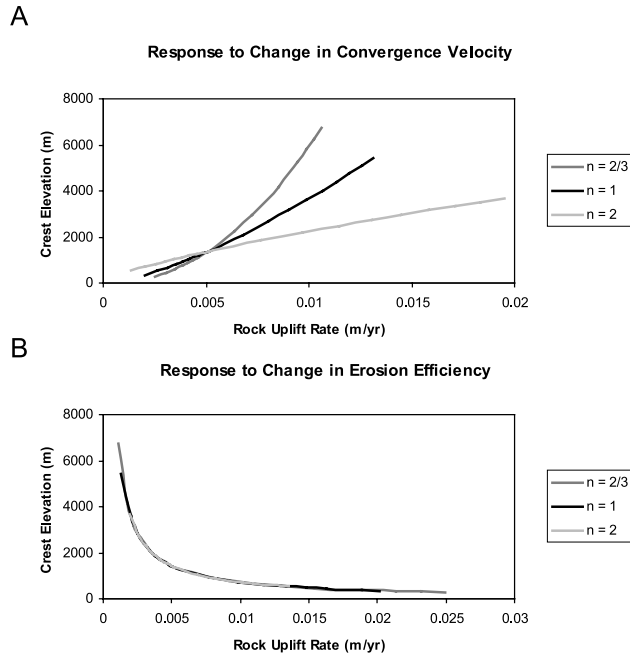


Figure 9. (a) Crest elevation (or, equivalently, topographic relief or wedge width) plotted against rock uplift rate (or, equivalently, erosion rate) as accretionary flux varies with erosional efficiency held constant, shown for different values of the slope exponent (n) from the stream power river incision model. (b) Crest elevation (or, equivalently, topographic relief or wedge width) plotted against rock uplift rate (or, equivalently, erosion rate) as erosional efficiency varies with accretionary flux held constant, shown for different values of the slope exponent (n) from the stream power river incision model.

reduces to K_p/K_r ($\tan \alpha_p/\tan \alpha_r$) $^{n-hm+qn-1}$ (assuming $\lambda \neq 1$ or, equivalently, that $K_r > 0$ as in this case the wedge would grow without bound; see equation (3a)):

$$W_r \propto W_p \propto K_p^0 K_r^{\frac{1}{hm+1-qn}}, \quad (28a)$$

$$U_r \propto K_p^0 K_r^{\frac{1}{hm+1-qn}}, \quad (28b)$$

$$U_p \propto K_p K_r^{\frac{hm-qn}{hm+1-qn}}. \quad (28c)$$

Note that equations (28a) and (28c) have the same form as equations (24) and (25) for the case $K_p = K_r$, respectively, as required.

[43] Interestingly, in this scenario ($\xi = 1$) the width (or relief) of the orogen and the rock uplift rate on the retro-wedge are entirely dictated by the efficiency of erosion on the retro-wedge, and their sensitivity is identical to that of either a one-sided wedge or one in which erosional efficiency is uniform. This may at first seem counterintuitive because the total accretionary flux into the system is obviously very sensitive to the erosional efficiency on the pro-wedge. However, the influence of the additional influx due to

recycling is completely absorbed in the pro-wedge itself (for $\xi = 1$, $F_{E_r} = F_{A_0}$ for all combinations of K_p and K_r): There is therefore a direct, linear relationship between steady state rock uplift rate and erosional efficiency on the pro-wedge (K_p). As a result, the retro-wedge is completely unaffected by erosion on the pro-wedge (equations (28a) and (28b)). Conversely, U_p actually decreases strongly with increasing K_r , despite the commensurate reduction in wedge width (equations (28a) and (28b)), because enhanced erosion on the retro-wedge reduces λ and therefore strongly reduces the total mass flux into the orogen (equation (3a)).

[44] For all other cases ($\xi \neq 1$), equations (24) and (25) do not reduce to power law functions of K_p and K_r . From inspection of equations (24)–(28) and Figure 10, we find that for typical values of h , m , n , and q , nonuniform erosional efficiency results in (1) a reduction of the sensitivity of orogen width (relief) and retro-wedge rock uplift rate to K_p (slight reduction for $\xi = 0$, extreme for $\xi = 1$) and K_r (moderate reduction for $\xi = 0$, no reduction for $\xi = 1$), (2) an increase in the sensitivity of pro-wedge rock uplift rate to K_p (slight increase for $\xi = 0$, extreme for $\xi = 1$), (3) an increase in the sensitivity of retro-wedge rock uplift rate to K_r (moderate increase for $\xi = 0$, no increase for $\xi = 1$), and (4) a reversal to an inverse relation (power law with negative exponent) between pro-wedge rock uplift rate and K_r (weakly inverse for $\xi = 0$, strongly inverse for $\xi = 1$). U_p decreases in response to an increase in K_r , even for $\xi = 0$, because the decrease in the fraction of material eroded off the pro-wedge (λ) is greater than the decrease in W_p : Material flux is very strongly drawn to the retro-wedge in response to an increase in K_r . In general, for $\xi \ll 1$, whereas wedge width (and therefore topographic relief) is most sensitive to K_p , retro-wedge rock uplift rate is most sensitive to K_r . An interesting implication is that for $\xi \ll 1$, it is plausible that a concentration of erosion on the retro-wedge (i.e., decreasing rainfall on the pro-wedge while increasing rainfall on the retro-wedge) could result in both an increase in retro-wedge rock uplift rate and a slight increase in topographic relief.

7. Kinematic Solution for Particle Velocities Within the Wedge

[45] In this section we present a generalization of *Dahlen's* [1988] analytical kinematic solution for the velocity field within a deforming wedge at critical taper. This generalization consists of an extension to nonuniform erosion (either increasing or decreasing toward the crest of the range) and to a two-sided wedge rather than the one-sided wedge of *Dahlen's* solution. The solution presented here is similar to that by *Pazzaglia and Brandon* [2001] and *Batt et al.* [2001] for a one-sided wedge. The extension to a two-sided wedge is achieved by solving for two back-to-back wedges that, in combination, are in steady state (material passes out the back of the pro-wedge and into the retro-wedge). The predicted velocity field provides a powerful illustration of the influence of the K_p/K_r ratio on particle trajectories through, and strain partitioning within, the deforming wedge. Differences in the internal velocity field give rise to different particle paths and thus different pressure-temperature-time histories, which are also best illustrated using this kinematic solution [see *Barr and*

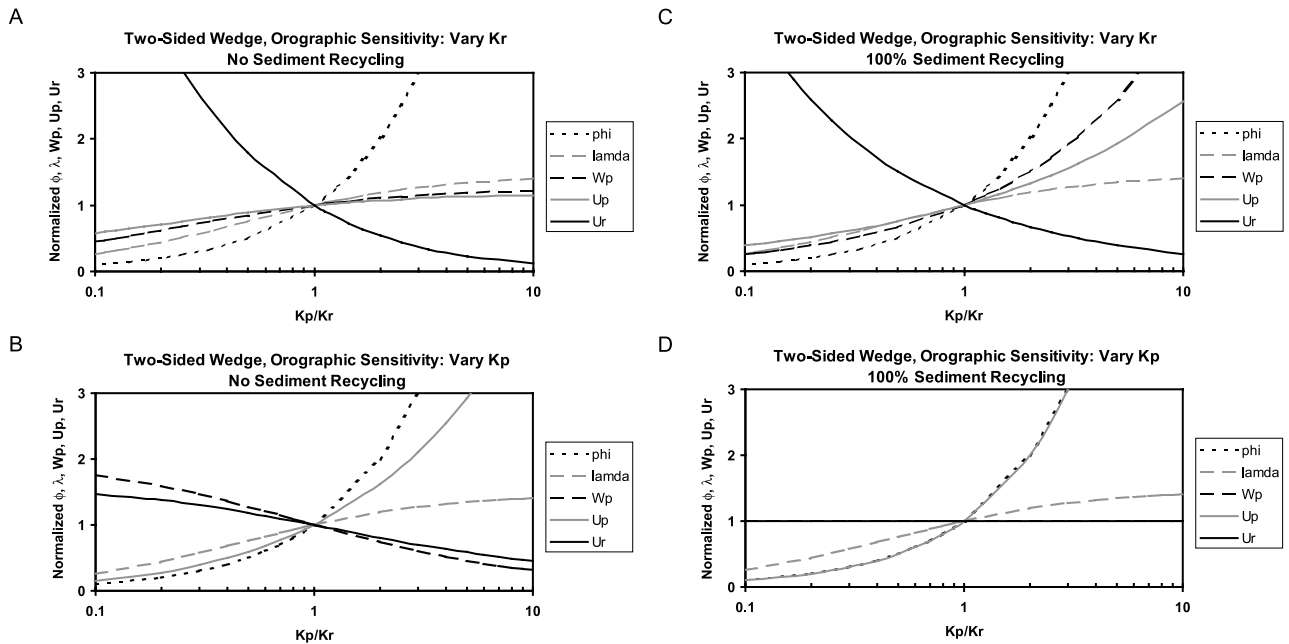


Figure 10. Two-sided wedge sensitivity to the orographic distribution of precipitation or differences in rock erodibility (K_p/K_r ratio). (a) $\xi = 0$ (no sediment recycling), K_r variable. (b) $\xi = 0$ (no sediment recycling), K_p variable. (c) $\xi = 1$ (complete recycling), K_r variable (see equation (28)). (d) $\xi = 1$ (complete recycling), K_p variable (see equation (28)). All variables are normalized to their value at $K_p/K_r = 1$.

Dahlen, 1989; Dahlen and Barr, 1989; Dahlen and Suppe, 1988]. Moreover, while section 6 relied on the assumption of spatially uniform erosion, the relaxation of that constraint allowed here lets us qualitatively explore the implications of various factors that could arguably cause a nonuniform distribution of erosion, such as intrabasin orographic precipitation patterns [Roe *et al.*, 2002, 2003], sediment flux and grain size controls on river incision rates [Sklar and Dietrich, 1998, 2001; Tomkin *et al.*, 2003; van der Beek and Bishop, 2003; Whipple and Tucker, 2002], debris flow scour [Stock and Dietrich, 2003], and possible glaciation at high elevation.

[46] Dahlen [1988] used a simple kinematic method to calculate the velocity everywhere in a deforming shallow taper wedge with erosion and no underplating. He took advantage of a somewhat simplified wedge geometry, assuming that the material enters the wedge at the toe, parallel to the surface slope. Thus our coordinate system for this calculation is aligned along the top surface of the wedge. Following Dahlen [1988], we use a slightly modified pro-wedge geometry with width ($W'_p = W_p - x_0$), total toe thickness (H'), and a total taper equal to the sum of the surface and basal slopes ($\alpha + \beta$) such that $x_0 = H'/\tan(\alpha + \beta)$ (Figures 3 and 11). Material enters the wedge through the toe at a rate V_x and exits through the top according to the specified erosion pattern $E(x)$. Total toe thickness H' includes any recycled material derived from erosion off the pro-wedge such that $F_A = H'V_x$ (see equation (3) and Figure 11). We consider power law erosion patterns with the forms $E(x) = \gamma(x - x_0)^c$ and $E(x) = \gamma(W' + x_0 - x)^c$ for erosion rate increasing and decreasing toward the divide, respectively, where c is the power law exponent and γ is the erosion intensity parameter ($\text{m}^{1-c} \text{yr}^{-1}$), chosen such that

the average erosion rate between x_0 and $x_0 + W'$, $\bar{E} = \gamma(c + 1)^{-1}(W')^c$ (for either case), equals U_p (equation (25)) and similar for the retro-wedge. Note that for all calculations here, x_0 is very small such that mass balance is maintained. The purpose of introducing this relation is to explore the consequences of a nonuniform pattern of erosion; mean erosion rates are still governed by the orogen-scale erosion rule developed above (equation (23)). Thus with the uniform erosion assumption used earlier now relaxed, the statement of mass balance for the two-sided wedge (equation (2)) can be rewritten:

$$\gamma_p = \frac{(c + 1)\lambda F_A}{(W_p - x_0)^{c+1}}; \quad \gamma_r = \frac{(c + 1)(1 - \lambda)F_A}{W_r^{c+1}}, \quad (29)$$

where W_p is given by equation (24) and W_r can be derived by combining equations (24) and (4). Equation (29) reduces to equation (2) for uniform erosion ($c = 0$) and $x_0 = 0$, as required.

[47] Following Dahlen [1988], we can calculate the velocity in a thin wedge of material by conserving mass and matching velocity boundary conditions. We assume that the wedge material is incompressible and that the density is constant in time and space. Thus we can write mass conservation as

$$\frac{\partial u}{\partial x} + \frac{\partial v}{\partial y} = 0, \quad (30)$$

where u and v are the horizontal and vertical components of the velocity field, respectively. At steady state the amount of material coming in should be equal to the amount eroded off the top. For the case of the one-sided wedge considered by

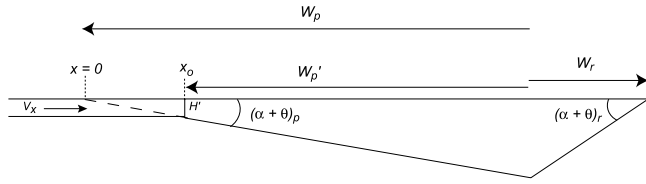


Figure 11. Definition sketch for kinematic model of internal deformation of a two-sided wedge, after *Dahlen* [1988] and *Dahlen and Suppe* [1988]. Note that H' includes any recycled material eroded off the pro-wedge such that $F_A = H'V_x$. $\alpha + \beta$ is the total taper of the wedge, which is approximated for the kinematic solution only as having no surface topographic expression.

Dahlen [1988], but with a power law distribution of erosion, this mass balance constraint can be written as

$$F_A = \int_{x_0}^{x_0+W'} \gamma(x-x_0)^c dx = \frac{\gamma W'^{c+1}}{c+1}, \quad (31)$$

where F_A includes any recycled sediment eroded off the pro-wedge (equation (3)). For the case of uniform erosion ($c = 0$) treated by *Dahlen* [1988], equation (31) reduces to $F_A = \dot{e}W'$, where we have set $\gamma = \dot{e}$ to coincide with *Dahlen's* [1988] notation. The case with $c = 1$ for a one-sided wedge was treated by *Dahlen and Suppe* [1988] and *Dahlen and Barr* [1989]. We will return to the question of mass balance for a two-sided wedge below.

[48] The horizontal velocities at the boundaries are satisfied by

$$F_A = \int_{x_0}^x \gamma(x' - x_0)^c dx' + ux(\alpha + \beta) = \frac{\gamma(x - x_0)^{c+1}}{c+1} + ux(\alpha + \beta) \quad (32a)$$

and

$$F_A = \int_{x_0}^x \gamma(W' + x_0 - x')^c dx' + ux(\alpha + \beta) = -\frac{\gamma}{c+1} [(W' + x_0 - x)^{c+1} - W'^{c+1}] + ux(\alpha + \beta) \quad (32b)$$

for erosion rate increasing and decreasing toward the divide, respectively. Equations (32a) and (32b) ensure that the horizontal velocity at the toe is the same as the input velocity $u(x = x_0) = V_x$ and that it vanishes when all material accreted at the toe has been eroded. Here we have made the shallow taper approximation $H'/x_0 = \tan(\alpha + \beta) \approx \alpha + \beta$ for small $\alpha + \beta$ and have assumed that there is no vertical variation in u , the horizontal component of the velocity field. Again, equation (32) is a more general form of *Dahlen's* [1988] uniform erosion formulation $F_A = \dot{e}(x - x_0) + ux(\alpha + \beta)$. We can find the horizontal velocity field

inside the wedge by solving equation (32) for $u(x)$. This gives

$$u(x) = \frac{F_A - \gamma(c+1)^{-1}(x-x_0)^{c+1}}{x(\alpha + \beta)} \quad (33a)$$

and

$$u(x) = \frac{F_A + \gamma(c+1)^{-1}[(W' + x_0 - x)^{c+1} - W'^{c+1}]}{x(\alpha + \beta)} \quad (33b)$$

for erosion rate increasing and decreasing toward the divide, respectively. After differentiating equation (33) with respect to x and substituting the result into equation (30), we can solve equation (30) for $\partial v/\partial y$, integrate with respect to y , and apply the top surface boundary condition $v(x, y = 0) = -\gamma(x - x_0)^c$ or $v(x, y = 0) = -\gamma(W' + x_0 - x)^c$ to give the vertical component of the velocity field:

$$v(x, y) = \frac{x^{-2}F_A - \gamma(c+1)^{-1}x^{-1}(x-x_0)^c [x^{-1}(x-x_0) - (c+1)]}{\alpha + \beta} \cdot y - \gamma(x-x_0)^c \quad (34a)$$

and

$$v(x, y) = \frac{\gamma(W' + x_0 - x)^c}{(\alpha + \beta)x} y + \frac{F_A + \frac{\gamma}{c+1} [(W' + x_0 - x)^{c+1} - W'^{c+1}]}{(\alpha + \beta)x^2} y - \gamma(W' + x_0 - x)^c \quad (34b)$$

for erosion rate increasing and decreasing toward the divide, respectively.

[49] At this point in the solution for the velocity field we have yet to insist that the wedge as a whole is at steady state. If we enforce steady state for a one-sided wedge by substituting in equation (31), equation (34) reduces to *Dahlen's* [1988] solution for the case of uniform erosion ($c = 0$; $\gamma = \dot{e}$). Retaining the general formulation of equation (34) that does not require steady state for a one-sided wedge, however, allows us to combine the solution for two back-to-back wedges (where material may pass through the back of the pro-wedge and into the retro-wedge) to find the solution for a two-sided wedge at steady state.

[50] To model the internal deformation of a two-sided wedge, we combine the solutions for two nonsteady state wedges. The approach allows us to maintain a solution where the horizontal velocities vary smoothly, while the vertical velocities may accommodate rather abrupt changes in response to the change in erosion pattern where the two wedges meet. We enforce mass balance for the whole system; that is, the input flux is balanced by the flux of material out of the top of the model, regardless of the spatial pattern of erosion. The total mass balance for a two-sided wedge is given by equation (29) above. For simplicity, we consider the case where accretionary influx is entirely into the pro-wedge side (see Figure 11).

[51] We now have enough relations to ensure that mass is balanced in the system so long as the geometry of the two wedges is compatible. We make sure that this is the case by

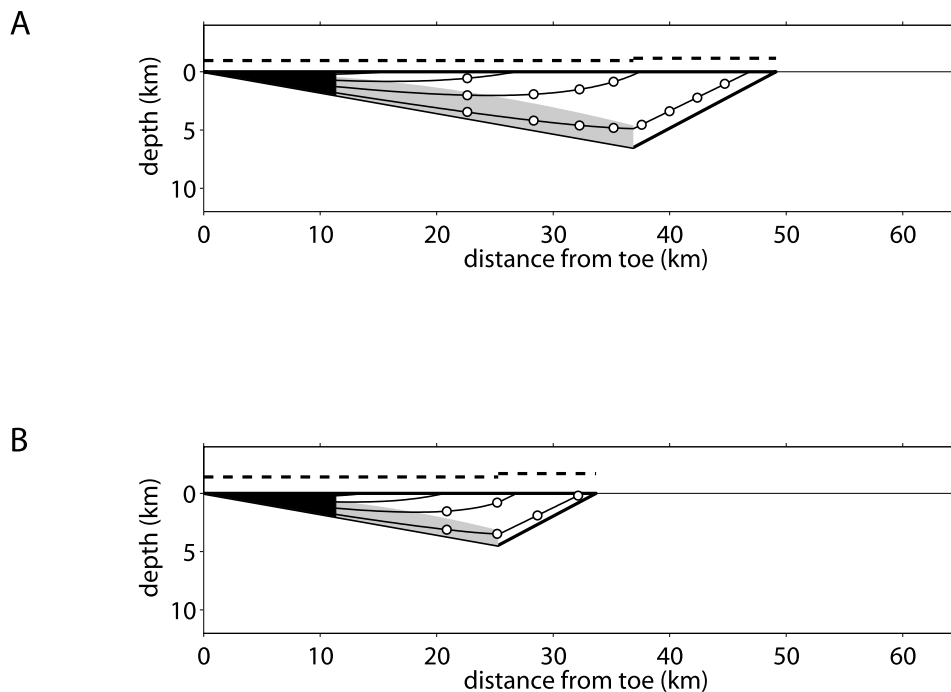


Figure 12. Internal velocity field and integrated particle trajectories for $K_p/K_r = 1$ and uniform erosion patterns ($c = 0$). In all cases shown in Figures 12–14 the following conditions hold: $(\alpha + \beta)_p = 10^\circ$, $(\alpha + \beta)_r = \sim 35^\circ$, $F_A = 50 \text{ m}^2 \text{ yr}^{-1}$, $n = 1$, $m = 0.5$, $K = 0.00001 \text{ yr}^{-1}$, $q = 0$, $k^* = 1$, $h = 1.67$, $k_a = 6.69$, dots along particle trajectories demarcate 1 Ma time intervals, relative erosion rates are plotted as height above the surface (dashed lines), zone of downward particle velocities (active burial) is shaded gray, particle paths are not computed within the black-shaded wedge tip (note, however, x_0 is a small fraction of the black shaded region), and plots have no vertical exaggeration. (a) Reference case for comparison to all other solutions. (b) Uniform increase in precipitation (or reduction of rock strength): doubling of both K_p and K_r relative to the reference case.

insisting that the heels of the two wedges meet at the deepest part (Figure 11):

$$H'_p + W'_p \tan(\alpha + \beta)_p = W_r \tan(\alpha + \beta)_r. \quad (35)$$

For the scenario considered here, there is no influx through the toe of the retro-wedge, so we typically let $H'_r = 0$. With the relationships defined above we can construct the velocity field inside a steady state two-sided wedge for both uniform ($c = 0$) and power law erosion cases. We can then readily integrate numerically to calculate particle paths and derive pressure-time histories for two-sided orogens. This could be coupled with equations for the steady state temperature distribution to determine the full pressure-temperature-time histories for particles traveling through this type of wedge [see *Barr and Dahlen, 1989; Barr et al., 1991; Batt and Brandon, 2002; Batt et al., 2001; Dahlen and Suppe, 1988*]. Although we have assumed here that both sides of the wedge experience the same type of erosion pattern, this constraint can be relaxed by replacing the common c with a separate one for both the pro-wedge and retro-wedge.

[52] Figures 12–14 illustrate the relation between the pattern of erosion (pro-wedge versus retro-wedge erosivity reflecting orographic focusing; uniform versus nonuniform

erosion) and particle trajectories through the orogen and are discussed in section 8.

8. Discussion

8.1. Orogen-Scale Erosion Rule

[53] The orogen-scale erosion rule derived here (equation (23)) is a general result that is potentially useful for one-dimensional coupled tectonic and surface process geodynamic models such as those developed by *Beaumont et al. [1996]*, *Willett [1999a]*, and *Beaumont et al. [2001]*. Derivation of equation (23) is the first formal defense of an erosion rule in which regional denudation rates are proportional to the mean topographic gradient at orogen scale. It is important to note here that the erosion rate depends on the orogen-perpendicular width of the erosional front (i.e., the size of the drainage basins with headwaters at the divide [see *Hovius, 1996*]) but does not necessarily increase with distance from the divide, as is sometimes assumed [*Hilley et al., 2004; Willett, 1999a*], because increasing drainage area is offset by decreasing channel gradient. As mentioned in section 5.2, it is inappropriate to simply apply rules developed for bedrock channels to a mean topographic profile without defining the relation between channel longitudinal profiles and the mean topographic gradient; doing so will impart a strong spatial pattern to erosion rates that is unrelated to any physical processes. As shown in

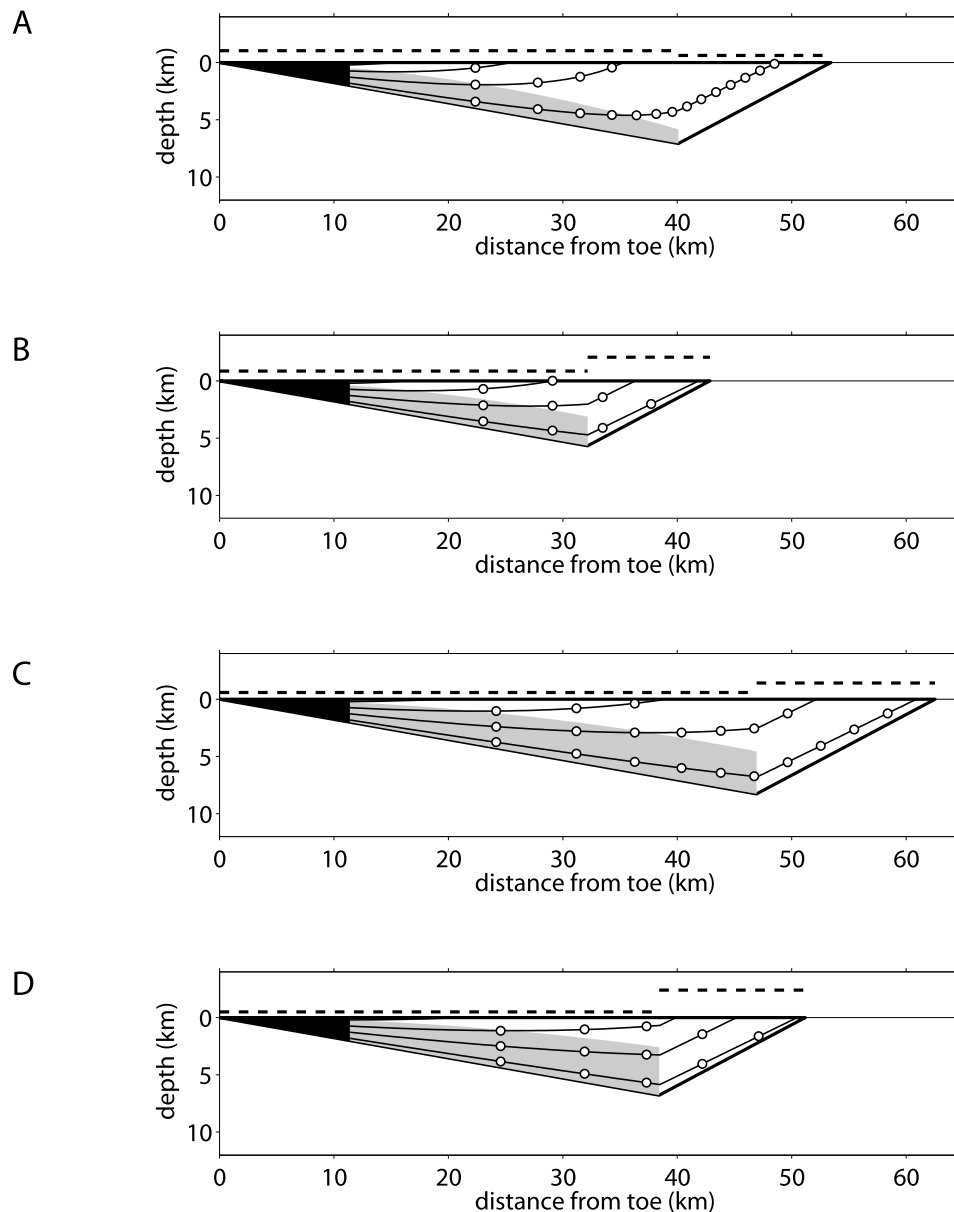


Figure 13. Internal velocity field and integrated particle trajectories for $K_p/K_r \neq 1$ and uniform erosion patterns ($c = 0$). See Figure 12 and caption for reference case and standard wedge geometry. (a) Dry (or resistant) retro-wedge ($K_r = 0.5$ *standard; $K_p/K_r = 2$). (b) Wet (or weak) retro-wedge ($K_r = 2$ *standard; $K_p/K_r = 0.5$). (c) Dry (or resistant) pro-wedge ($K_p = 0.5$ *standard; $K_p/K_r = 0.5$). (d) Dry (or resistant) pro-wedge ($K_p = 0.5$ *standard) and wet (or weak) retro-wedge ($K_r = 2$ *standard; $K_p/K_r = 0.25$).

section 7, the erosion rate pattern can importantly influence many aspects of orogen evolution, and care is required in the formulation of models that predict spatially nonuniform erosion in steady state orogenic wedges: It is important to get the right pattern and for the right reasons. Further, the nonlinearity of the relationship between denudation rate and mean topographic gradient is dictated by the mechanics of the processes of bedrock channel erosion and internal feedbacks among topography, incision rate, and the efficiency of incision [Hancock *et al.*, 1998; Roe *et al.*, 2002, 2003; Snyder *et al.*, 2000, 2003a, 2003b; Tucker, 2004; Whipple *et al.*, 2000; Whipple and Tucker, 1999]. Further, it is worth noting that our finding that higher erosion and rock uplift rates are expected on the retro-wedge under uniform climatic and

lithologic conditions implies that orogen-scale erosion rate is not simply dependent on topographic relief but that it depends more strongly on the mean topographic gradient than on orogen width (i.e., $b > a$ in equation (5), the general erosion rule posited in section 4.3).

8.2. Coupling With Feedback Among Climate, Erosion, and Tectonics

[54] As noted by previous workers, there is a strong, direct coupling between climate (or erosional efficiency) and tectonics [Avouac and Burov, 1996; Beaumont *et al.*, 1992, 2001; Dahlen and Suppe, 1988; Koons, 1995; Koons *et al.*, 2002; Willett, 1999a]. Our analysis has demonstrated the fundamental nature of this coupling and has quantified

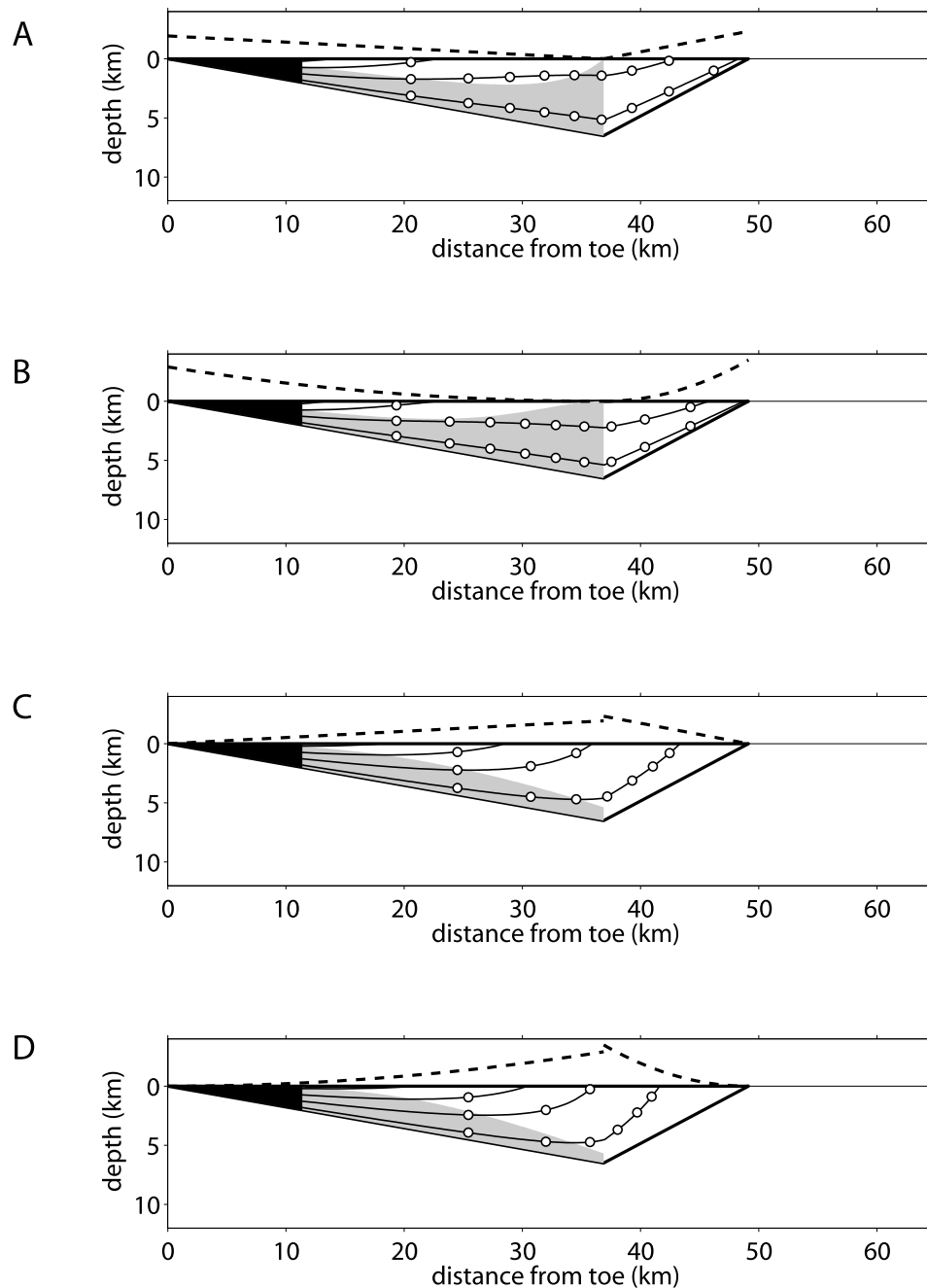


Figure 14. Internal velocity field and integrated particle trajectories for nonuniform erosion patterns ($c \neq 0$) but with $K_p/K_r = 1$. See Figure 12 and caption for reference case and standard wedge geometry. (a) Erosion decreasing linearly toward the divide ($c = 1$). (b) Erosion decreasing nonlinearly toward the divide ($c = 2$). (c) Erosion increasing linearly toward the divide ($c = 1$). (d) Erosion increasing nonlinearly toward the divide ($c = 2$).

its strength in frictional orogens, at least to first order. Although erosion does not build mountains, it does fundamentally influence the size, shape, and geodynamics of active orogens. At orogen scale, erosion drives rock uplift. This statement is explicitly limited to isostatically compensated orogenic wedges and cannot in general be said for rock uplift on single structures such as occurs in some well-studied field areas such as the King Range [Merritts and Bull, 1989; Merritts and Vincent, 1989; Snyder *et al.*, 2000,

2003a], the San Gabriel Mountains [Blythe *et al.*, 2000], the Siwalik Hills [Hurtrez *et al.*, 1999; Kirby and Whipple, 2001; Lague and Davy, 2003; Lavé and Avouac, 2000], and Wheeler Ridge [Keller *et al.*, 1998, 2000; Mueller and Suppe, 1997]. Steady state orogen width, cross-sectional area, and topographic relief are equally controlled by the inverse of the erosional efficiency ($1/K$) and by the accretionary flux (F_A) (equations (24) and (27a); Figures 7a and 8a). Remarkably, steady state rock uplift rate is more

strongly controlled by erosional efficiency than by the accretionary flux for most values of the erosion law exponents h , m , and n (equations (25) and (27b); Figures 7b and 8b). However, internal feedbacks among topography, incision rate, and the efficiency of incision (e.g., narrowing of channel width in response to rapid incision, changes in channel bed state, orographic enhancement of precipitation, diminishing importance of the critical shear stress for incision at high incision rates, etc.) will act to dampen the coupling among orogen size, rock uplift rate, and erosional efficiency. Thus it can be said that for a given tectonic setting and material properties, climate, or, more precisely, erosional efficiency, controls steady state orogen width, range crest elevation, topographic relief, crustal thickness, and rock uplift rate. Moreover, the details of the active erosion processes are clearly important as their nonlinearity governs both the relation between climate variables and K and the sensitivity of wedge width, relief, and rock uplift rate to both K and the accretionary flux F_A (see equations (24)–(27a); Figures 7–9).

[55] An increase in steady state rock uplift rate in response to a more erosive climate, however, does not indicate an increase in the total erosional efflux, which by definition just balances the incoming accretionary flux (with the only complication that the total accretionary flux includes the fraction of eroded material that is recycled back into the orogenic wedge (see equation (3a))). Erosionally induced enhancement of rock uplift rate occurs only by focusing deformation, be it through narrowing the orogen or through concentrating deformation either in a weakened shear zone [e.g., *Beaumont et al.*, 1996] or on one side of orogen or the other in response to prevailing winds and the resulting orographic distribution of precipitation [e.g., *Willett*, 1999a]. Given that for a given accretion rate, faster rock uplift rates are associated with narrower orogens, steady state topographic relief is reduced in response to an increase in erosional efficiency (K), despite the commensurate increase in rock uplift rate (Figures 8a and 9b). This finding generalizes and extends the analysis of *Whipple et al.* [1999]. There are two possible exceptions: (1) if $\xi = 1$, whereas steady state relief is independent of pro-wedge erosional efficiency (K_p), pro-wedge rock uplift rate increases linearly with K_p ; (2) if an increase in erosional efficiency on the retro-wedge is combined with a decrease on the pro-wedge, it is possible that wedge size and topographic relief increase (or remain constant), despite the accelerated rate of erosion on the retro-wedge (only possible for $\xi \sim 0$). A scenario illustrative of the latter is shown in Figure 13d (compare to Figure 12a). Any such increase in topographic relief is minor (a few percent maximum), however, and is only allowed by a very narrow range of conditions.

8.3. Sedimentation Rates and the Role of Quaternary Climate Change

[56] The past decade has seen much interest in the possible influences of Quaternary climate change on erosion, sedimentation rates, and topographic relief [e.g., *Brocklehurst and Whipple*, 2002; *Brozovic et al.*, 1997; *Gilchrist and Summerfield*, 1991; *Gilchrist et al.*, 1994; *Molnar*, 2001; *Molnar and England*, 1990; *Montgomery*, 1994, 2002; *Montgomery and Greenberg*, 2000; *Roe et al.*,

2003; *Schmidt and Montgomery*, 1995; *Small and Anderson*, 1995, 1998; *Whipple et al.*, 1999; *Zhang et al.*, 2001]. Here we describe implications of our findings for this debate. First, although a change in climate cannot change total steady state erosional efflux from an active orogen, the transition from one steady state condition to another will involve a considerable change in the cross-sectional area of the orogenic wedge (wedge cross-sectional area $\sim W^2 \sim K^{-(0.8-1.4)}$). Thus a potentially large volume of “excess” sediment will be produced in response to a change in erosional efficiency (K). The commensurate increase in the sedimentation rate depends on the system response timescale [*Kooi and Beaumont*, 1996; *Pazzaglia and Brandon*, 1996; *Whipple*, 2001; *Whipple and Tucker*, 1999]. This provides a plausible explanation for the heightened sedimentation rates in some areas during the Quaternary cited by *Molnar and England* [1990] and *Zhang et al.* [2001]. However, if Quaternary climate change produced a significant increase in erosivity (due to the onset of glaciation, oscillations between glacial and nonglacial climates, increased storminess, etc.), our model predicts that active orogenic wedges should have been shrinking during the Quaternary at a rate commensurate with the excess sediment produced. This constitutes a testable hypothesis (past orogen widths should prove more easily determined than paleoelevation), at least in principle. Further, the total amount of excess sediment produced potentially provides a constraint on the change in wedge volume and therefore the magnitude of the effective change in erosional efficiency (K) associated with Quaternary climate change.

8.4. Sensitivity to the Orographic Distribution of Rainfall

[57] Our analysis has shown that the relative efficiency of erosion on the pro-wedge and retro-wedge sides of the orogen (K_p/K_r ratio) exerts a fundamental control on steady state wedge width, topographic relief, and patterns of internal deformation within the wedge (Figures 10 and 13). Equations (26) and (9) show that the relative rates of exhumation on the pro-wedge and retro-wedge sides of the orogen are governed directly by the K_p/K_r ratio, which is determined in part by the orographic distribution of precipitation on windward versus leeward slopes and in part by rock strength, which itself is influenced by particle paths through the orogen and the associated patterns of internal deformation. As discussed in section 6.2, system sensitivity to the orographic distribution of precipitation is also importantly influenced by the efficiency of sediment recycling into the orogen (restricted to the pro-wedge in our analysis) (compare equations (27) and (28)). This follows because the erosional efflux off the pro-wedge feeds back into the total accretionary flux (see equation (3a)). In the extreme case of total recycling ($\xi = 1$), there is a direct, linear, causative relation between pro-wedge erosional efficiency (K_p) and the pro-wedge rock uplift rate (equation (28)). If $\xi = 1$, however, the retro-wedge erosional efflux must equal the far-field tectonic influx (F_{A_0}) for all combinations of K_p and K_r . Accordingly, in this scenario, wedge width, range crest elevation, topographic relief, and retro-wedge rock uplift rate are all dictated directly by K_r , the erosional efficiency on the retro-wedge (K_p has no influence).

[58] The influence of the macroscale pattern of erosion (pro-wedge versus retro-wedge erosion rate) is best illustrated by the changing patterns of internal deformation, as shown by our kinematic solution for the velocity field within the wedge (Figures 12a and 13). The relative rates of exhumation on the pro-wedge and retro-wedge naturally dictate the percentage of the total accretionary flux that is eroded off either side of the orogen (equation (9)). This, in turn, dictates the mass flux pattern and therefore for frontal accretion, governs particle trajectories, P - T - t paths, and the pattern of exposed rocks in terms of metamorphic grade [e.g., Barr and Dahlen, 1989; Barr et al., 1991; Beaumont et al., 1992; Dahlen and Suppe, 1988; Jamieson and Beaumont, 1988; Koons, 1987], as illustrated in Figures 12a and 13. A component of underplating, and its spatial distribution, could readily be added and would clearly also exert first-order control on particle trajectories and P - T - t paths [e.g., Barr and Dahlen, 1989; Batt and Brandon, 2002; Dahlen and Barr, 1989; Willett et al., 2001].

8.5. Sensitivity to Spatially Nonuniform Erosion

[59] Our mass balance formulation was written in terms of the average rock uplift rate on the pro-wedge and retro-wedge sides of the orogen. The relations we used for equilibrium topography are strictly for uniform rock uplift and therefore for uniform erosion rates on either side of the orogen. Whereas this is consistent with typical stream concavity indices (θ in equation (10)) and simple fluvial erosion models ($\theta = m/n$ for uniform erosion and the stream power incision model used here), many factors may cause erosion rates to vary systematically downstream along river profiles with typical concavity indices (note that typical river concavities and network topologies are consistent with a linear mean topographic profile (see Figure 5)). These factors include (1) the intrabasin distribution of orographic precipitation [Roe et al., 2002, 2003]; (2) the frequency of occurrence of erosive debris flows in channel headwater segments [Stock and Dietrich, 2003]; (3) changing sediment size and/or supply relative to carrying capacity with distance downstream [Sklar and Dietrich, 1998, 2001; Tomkin et al., 2003; van der Beek and Bishop, 2003; Whipple and Tucker, 2002]; (4) controls on channel width [Hancock and Anderson, 2002; Montgomery and Gran, 2001; Suzuki, 1982]; and (5) highly efficient erosion associated with possible glaciation in headwater channel reaches [Brocklehurst and Whipple, 2002; Hallet et al., 1996; MacGregor et al., 2000]. We have qualitatively illustrated the potential orogen-scale influence of these “details” of the erosion process through our kinematic solution for the deformation within the orogenic wedge by relaxing the assumption of a spatially uniform erosion rate. Figures 12a and 14 demonstrate that realistic patterns of nonuniform erosion can significantly alter the internal deformation field and resulting rock particle P - T - t paths. This result strongly underscores the point raised earlier that the details of the erosion process may significantly influence orogen evolution. Most coupled tectonic and surface process models of orogen evolution use highly simplified erosion rules and are therefore somewhat limited in their predictive capability in this regard. However, many questions remain about the long-term modeling of erosion, particularly as regards the above list of factors influencing

the spatial pattern of erosion. Further field and laboratory study of these key issues is greatly needed.

8.6. Limitations

[60] Assumptions required in an analytical model such as that presented here necessarily sacrifice generality for clarity. There are important limitations to our model, both in terms of the tectonic and erosional aspects of the formulation. First and foremost, the strict adherence to the self-similar geometry of frictional orogenic wedges at critical taper is an end-member model, particularly given our insistence that topographic taper be held invariant with climate, accretionary flux, and wedge width. Systematic variations in topographic taper with any of these variables could change system response to first order. For example, if there is a fixed rooting depth of the basal decollement, one expects the slope of the decollement to decrease linearly with wedge width [Hilley et al., 2004]. As a shallower decollement requires a steeper topographic taper [Dahlen, 1984], this circumstance can be anticipated to cause steady state erosion rate to increase more rapidly with wedge width than in the constant decollement slope scenario considered here [Hilley et al., 2004]. The implication is that exponents in equations (5)–(8) and (24)–(27a) would be changed somewhat (generally replace a with $a + 1$ or $hm - qn + 1$ with $hm - qn + 2$). Similarly, it is plausible that pore pressures on the basal decollement vary with climate and/or wedge width in a manner similar to that discussed by Saffer and Bekins [2002] for submarine accretionary prisms. Another important consequence of self-similar wedge growth is that the asymmetry of the orogen is set; the orographic distribution of precipitation can influence wedge size, rock uplift rate, and strain partitioning within the wedge but cannot cause migration of the drainage divide, as has been discussed by Montgomery et al. [2001] for the Andes and by Willett [1999a] and Willett et al. [2001] on the basis of numerical simulations. The difference with the model of Willett et al. [2001] is that while they proscribe the uplift pattern and solve for wedge geometry free from mechanical constraints, we enforce critical taper geometry (holding basal decollement angle and frictional properties constant) and solve for the deformation pattern, rock uplift rate at the surface, and hence the U/V_x ratio that figures prominently in their analysis.

[61] The restriction to purely frictional mechanics is another important limitation of our analysis. We hasten to point out, however, that the restriction to invariant frictional properties is conservative; systems subject to positive feedback between erosion and rheology (for example, through a thermally activated viscosity) will exhibit even stronger coupling among climate, erosion, and deformation and therefore a more sensitive dependence on the erosion rule and the resulting pattern of erosion than shown here. Orogens like the Himalaya/Tibet system appear to be a prime example of this effect, as illustrated in recent numerical simulations by Beaumont et al. [2001] and Koons et al. [2002]. Even the archetypical Taiwan orogen is likely thick enough and hot enough to be influenced by viscous effects not modeled here [Willett, 1999b; Willett et al., 1993]. The analytical solution presented here, however, may provide an opportunity to systematically explore the degree to which the onset of viscous deformation in the deeper and hotter

parts of the orogenic wedge influence the nature and strength of the feedbacks among climate, erosion, and tectonics: The response of orogen width, rock uplift rate, and strain partitioning to imposed patterns of erosional efficiency predicted by existing coupled thermomechanical and surface processes models (if modified to use the orogen-scale erosion rule of equation (23) developed here) could be quantitatively compared with expectations for purely frictional wedges (equations (24)–(28)).

[62] Similarly, the stream power river incision model appears here as a simple, phenomenological placeholder for more sophisticated models currently under development. Many factors influence the effective values of the model parameters K , m , and n in complex and as yet not fully understood ways, involving adjustments in channel width [Montgomery *et al.*, 2002; Snyder *et al.*, 2003a], bed morphology [Massong and Montgomery, 2000], sediment grain size and abundance [Sklar and Dietrich, 1998, 2001; Whipple and Tucker, 2002], and the relative importance of extreme events [Snyder *et al.*, 2003b; Tucker, 2004; Tucker and Bras, 2000]. Importantly, the quantitative relationship between measurable climate parameters and K , the coefficient of erosion, remains elusive despite recent progress [Snyder *et al.*, 2003b; Tucker, 2004; Tucker and Bras, 2000], particularly given the short timescale of climate change. Although much is revealed by the present analysis in terms of these effective model parameters, there exists a real potential for different effective values of exponents m and n on either side of the orogenic wedge. Any such difference would change steady state wedge size and, in particular, strongly influence system sensitivity to the orographic distribution of precipitation (pro-wedge versus retro-wedge side erosional efficiency). Finally, the approximate empirical relationship between channel longitudinal profiles and the regional mean topographic gradient breaks down somewhat when relief is extreme and hillslopes/colluvial channels become a significant fraction of the total relief, as is evident in the data plotted in Figure 5. However, a slight nonlinearity in this relationship will not much influence the sensitivity of steady state wedge width and rock uplift rate to erosional efficiency and accretionary flux.

9. Conclusions

[63] Major conclusions drawn from this work and explored in some depth in the discussion include the following.

[64] 1. For a given tectonic setting (far-field tectonic influx and frictional material properties), erosional efficiency controls steady state orogen width, relief, crustal thickness, and rock uplift rate. System sensitivity to differences (or changes) in climate, rock properties, and accretionary flux is dictated by the details of the erosion law.

[65] 2. For uniform erosional efficiency ($K_p = K_r$), orogen width and topographic relief are equally sensitive to the inverse of the coefficient of fluvial erosion ($1/K$) and accretionary flux (F_A), scaling as power law relations with exponents in the range 0.4–0.7 for typical stream power river incision model parameters. Interestingly, rock uplift rate is actually more sensitive to erosional efficiency than to the accretionary flux for most combinations of model parameters ($U \sim K^{0.4-0.7} F_A^{0.3-0.6}$). However, the net steady state erosional efflux is, of course, unchanged. Net erosional

efflux only increases above the accretionary flux during transients in which an increase in erosional efficiency drives a reduction in the volume of material stored within the orogenic wedge.

[66] 3. The dynamic response of rock uplift rate to a change in erosional efficiency is due to a narrowing of the orogenic wedge and thus a focusing of exhumation. There can be no dynamic coupling between erosional efficiency and rock uplift rate in an orogen of fixed width experiencing homogeneous pure shear deformation.

[67] 4. As a direct consequence of the dynamic coupling between erosional efficiency and rock uplift rate in a critically tapered orogenic wedge, rock erodibility can influence steady state erosion rate, contrary to field settings where rock uplift rate is an independent, externally forced parameter. In this commonly assumed scenario, rock erodibility (and climate) can influence only steady state topographic form, not the steady state erosion rate [e.g., Whipple *et al.*, 1999].

[68] 5. With two exceptions, steady state topographic relief is always reduced by an increase in erosional efficiency, despite the commensurate increase in rock uplift rate. The two exceptions are (1) if $\xi = 1$, whereas steady state relief is independent of pro-wedge erosional efficiency (K_p), pro-wedge rock uplift rate increases linearly with K_p and (2) if an increase in erosional efficiency on the retro-wedge is combined with a decrease on the pro-wedge, it is possible that wedge size and topographic relief increase (or remain constant) despite the accelerated rate of erosion on the retro-wedge (only possible for $\xi \sim 0$).

[69] 6. If Quaternary climate change has been associated with a significant increase in erosional efficiency [Molnar, 2001; Molnar and England, 1990], a direct predictable consequence is that active, well-developed (i.e., not in the earliest stages of growth) orogenic wedges would have shrunk, or would be shrinking, in size and would have experienced real increases in rock uplift rate. Further, any extra volume of sediment produced during the Quaternary [Zhang *et al.*, 2001] in principle provides a constraint on the magnitude of the change in wedge cross-sectional area and therefore on the magnitude of the change in the efficiency of erosion (i.e., the change in K).

[70] 7. For frontal accretion with no underplating the K_p/K_r ratio (controlled by both climatic and rock property contrasts between the pro-wedge and retro-wedge) sets the deformation pattern, time-averaged particle trajectories through the orogen and thus P - T - t paths experienced during burial and then exhumation. In addition, nonuniform erosional efficiency ($K_p \neq K_r$) results in (1) a reduction of the sensitivity of orogen width (relief) and retro-wedge rock uplift rate to K_p (slight reduction for $\xi = 0$, extreme for $\xi = 1$) and K_r (moderate reduction for $\xi = 0$, no reduction for $\xi = 1$), (2) an increase in the sensitivity of pro-wedge rock uplift rate to K_p (slight increase for $\xi = 0$, extreme for $\xi = 1$), (3) an increase in the sensitivity of retro-wedge rock uplift rate to K_r (moderate increase for $\xi = 0$, no increase for $\xi = 1$), and (4) a reversal to an inverse relation (power law with negative exponent) between pro-wedge rock uplift rate and K_r (weakly inverse for $\xi = 0$, strongly inverse for $\xi = 1$).

[71] 8. Nonuniform erosion along channel profiles (i.e., more intense erosion concentrated near the range crest or near the toe of the wedge) importantly influences particle

paths, patterns of strain within the orogenic wedge, and, presumably, the width of reset zones of thermochronometers [see Batt *et al.*, 2001; Willett and Brandon, 2002].

Notation

A	upstream drainage area (m^2).
a	width exponent in general erosion rule.
b	gradient exponent in general erosion rule.
C	coefficient of erosion in general erosion rule ($\text{m}^{1-a} \text{yr}^{-1}$).
c	exponent in nonuniform erosion pattern rule.
E, \dot{e}	average erosion rate (myr^{-1}).
F_A	total accretionary flux per unit distance along strike ($\text{m}^2 \text{yr}^{-1}$).
F_{A_0}	far-field accretionary flux per unit distance along strike ($\text{m}^2 \text{yr}^{-1}$).
H	thickness of incoming plate involved in deformation (m).
H'	thickness of pro-wedge at $x = x_0$ (m).
h	distance exponent in Hack's law.
K	coefficient of fluvial erosion ($\text{m}^{1-2m} \text{yr}^{-1}$).
K'	coefficient of erosion in orogen-scale erosion rule ($\text{m}^{1-hm+qn} \text{yr}^{-1}$).
k_a	coefficient in Hack's law (m^{2-h}).
k_0	fluvial relief correction factor.
k^*	fluvial relief correction factor coefficient (m^{-q}).
k_1	proportionality constant between L and W .
k_2	proportionality constant between R_f/L and $\tan \alpha$.
k_s	steepness index ($\text{m}^{2\theta}$).
L	main stem channel length (m).
m	area exponent in stream power river incision model.
n	slope exponent in stream power river incision model.
q	fluvial relief correction factor exponent.
R_f	fluvial relief (m).
S	local channel gradient.
S_L	local channel gradient at the mountain front.
U	average near-surface rate of rock uplift relative to the geoid (myr^{-1}).
u	horizontal component of particle velocity within deforming wedge (myr^{-1}).
V_x	tectonic convergence velocity (myr^{-1}).
v	vertical component of particle velocity within deforming wedge (positive downward) (myr^{-1}).
W	plan view wedge width (m).
W'	plan view width of wedge within domain of kinematic solution (m).
x	horizontal position coordinate (m).
x_c	distance from divide to fluvial channel head (m).
x_0	length of truncated wedge tip in kinematic solution (m).
y	vertical position coordinate (positive downward) (m).
α	topographic taper angle (rad).
β	dip of basal decollement (rad).
χ	geometric coefficient, fluvial relief ($\text{m}^{hm/n-2m/n-q}$).
λ	fraction F_A eroded off pro-wedge.
ϕ	ratio of pro-wedge to retro-wedge rock uplift rate.
γ	erosion intensity parameter ($\text{m}^{1-c} \text{yr}^{-1}$).
θ	concavity index.
ξ	recycled fraction of material eroded off pro-wedge.

p subscript denotes pro-wedge variable.
 r subscript denotes retro-wedge variable.

[72] **Acknowledgments.** Discussions with Sean Willett, Chris Beaumont, and Peter Koons were strongly influential, and we thank them for their time and patience. The idea to initiate the analysis presented here grew out of these discussions and out of interactions with colleagues in the Canadian Institute for Advanced Research. The work was supported by grants from NASA (SENH-99-0209-0172) and the NSF (EAR-0003571). Comments by Robert Anderson, Mike Ellis, Greg Tucker, and an anonymous reviewer resulted in significant improvements to an earlier draft.

References

- Ahnert, F. (1970), Functional relationships between denudation, relief, and uplift in large mid-latitude drainage basins, *Am. J. Sci.*, **268**, 243–263.
- Avouac, J.-P., and E. B. Burov (1996), Erosion as a driving mechanism of intracontinental mountain growth, *J. Geophys. Res.*, **101**, 17,747–17,769.
- Barr, T. D., and F. A. Dahlen (1989), Brittle frictional mountain building: 2. Thermal structure and heat budget, *J. Geophys. Res.*, **94**, 3923–3947.
- Barr, T. D., F. A. Dahlen, and D. C. McPhail (1991), Brittle frictional mountain building: 3. Low-grade metamorphism, *J. Geophys. Res.*, **96**, 10,319–10,338.
- Batt, G. E., and M. T. Brandon (2002), Lateral thinking: 2-D interpretation of thermochronology in convergent orogenic settings, in *Low Temperature Thermochronology: From Tectonics to Landscape Evolution*, edited by B. P. Kohn, *Tectonophysics*, **349**, 185–201.
- Batt, G. E., B. P. Kohn, J. Braun, I. McDougall, and T. R. Ireland (1999), New insight into the dynamic development of the Southern Alps, New Zealand, from detailed thermochronological investigation of the Matakake Range pegmatites, in *Exhumation Processes: Normal Faulting, Ductile Flow and Erosion*, edited by U. Ring *et al.*, *Geol. Soc. Spec. Publ.*, **154**, 261–282.
- Batt, G. E., J. Braun, B. P. Kohn, and I. McDougall (2000), Thermochronological analysis of the dynamics of the Southern Alps, New Zealand, *Geol. Soc. Am. Bull.*, **112**(2), 250–266.
- Batt, G. E., M. T. Brandon, K. A. Farley, and M. Roden-Tice (2001), Tectonic synthesis of the Olympic Mountains segment of the Cascadia wedge, using two-dimensional thermal and kinematic modeling of the thermochronological ages, *J. Geophys. Res.*, **106**, 26,731–26,746.
- Beaumont, C., P. Fullsack, and J. Hamilton (1992), Erosional control of active compressional orogens, in *Thrust Tectonics*, edited by K. R. McClay, pp. 1–18, Chapman and Hall, New York.
- Beaumont, C., P. J. J. Kamp, J. Hamilton, and P. Fullsack (1996), The continental collision zone, South Island, New Zealand: Comparison of geodynamical models and observations, *J. Geophys. Res.*, **101**, 3333–3359.
- Beaumont, C., R. A. Jamieson, M. H. Nguyen, and B. Lee (2001), Himalayan tectonics explained by extrusion of a low-viscosity crustal channel coupled to focused surface denudation, *Nature*, **414**, 738–742.
- Blythe, A. E., D. W. Burbank, K. A. Farley, and E. J. Fielding (2000), Structural and topographic evolution of the central Transverse Ranges, California, from apatite fission-track, (U-Th)/He and digital elevation model analyses, *Basin Res.*, **12**, 97–114.
- Boyer, S. E. (1995), Sedimentary basin taper as a factor controlling the geometry and advance of thrust belts, *Am. J. Sci.*, **295**, 1220–1254.
- Brocklehurst, S., and K. Whipple (2002), Glacial erosion and relief production in the eastern Sierra Nevada, California, *Geomorphology*, **42**, 1–24.
- Brozovic, N., D. Burbank, and A. Meigs (1997), Climatic limits on landscape development in the northwestern Himalaya, *Science*, **276**, 571–574.
- Burbank, D. W., J. Leland, E. Fielding, R. S. Anderson, N. Brozovic, M. R. Reid, and C. Duncan (1996), Bedrock incision, rock uplift and threshold hillslopes in the northwestern Himalayas, *Nature*, **379**, 505–510.
- Dahlen, F. A. (1984), Noncohesive critical Coulomb wedges: An exact solution, *J. Geophys. Res.*, **89**, 10,125–10,133.
- Dahlen, F. A. (1988), Mechanical energy budget of a fold-and-thrust belt, *Nature*, **331**, 335–337.
- Dahlen, F. A. (1990), Critical taper model of fold-and-thrust belts and accretionary wedges, *Annu. Rev. Earth Planet. Sci.*, **18**, 55–99.
- Dahlen, F. A., and T. D. Barr Jr. (1989), Brittle frictional mountain building: 1. Deformation and mechanical energy balance, *J. Geophys. Res.*, **94**, 3906–3922.
- Dahlen, F. A., and J. Suppe (1988), Mechanics, growth, and erosion of mountain belts, in *Processes in Continental Lithospheric Deformation*, edited by S. P. J. Clark, B. C. Burchfiel, and J. Suppe, pp. 161–178, Geol. Soc. of Am., Denver, Colo.
- Dahlen, F. A., J. Suppe, and D. Davis (1984), Mechanics of fold-and-thrust belts and accretionary wedges: Cohesive Coulomb theory, *J. Geophys. Res.*, **89**, 10,087–10,101.

- Davis, D., J. Suppe, and F. A. Dahlen (1983), Mechanics of fold-and-thrust belts and accretionary wedges, *J. Geophys. Res.*, *88*, 1153–1172.
- England, P., and P. Molnar (1990), Surface uplift, uplift of rocks, and exhumation of rocks, *Geology*, *18*, 1173–1177.
- Flint, J. J. (1974), Stream gradient as a function of order, magnitude, and discharge, *Water Resour. Res.*, *10*, 969–973.
- Gilchrist, A. R., and M. A. Summerfield (1991), Denudation, isostasy and landscape evolution, *Earth Surf. Processes Landforms*, *16*, 555–562.
- Gilchrist, A. R., M. A. Summerfield, and H. A. P. Cockburn (1994), Landscape dissection, isostatic uplift, and the morphologic development of orogens, *Geology*, *22*, 963–966.
- Hack, J. T. (1957), Studies of longitudinal stream profiles in Virginia and Maryland, *U.S. Geol. Surv. Prof. Pap.*, *294-B*, 1–97.
- Hallet, B., L. Hunter, and J. Bogen (1996), Rates of erosion and sediment evacuation by glaciers: A review of field data and their implications, *Global Planet. Change*, *12*, 213–235.
- Hancock, G. S., and R. S. Anderson (2002), Numerical modeling of fluvial strath-terrace formation in response to oscillating climate, *Geol. Soc. Am. Bull.*, *114*, 1131–1142.
- Hancock, G. S., R. S. Anderson, and K. X. Whipple (1998), Beyond power: Bedrock river incision process and form, in *Rivers Over Rock: Fluvial Processes in Bedrock Channels*, *Geophys. Monogr. Ser.*, vol. 107, edited by K. Tinkler and E. E. Wohl, pp. 35–60, AGU, Washington, D. C.
- Hilley, G. E., and M. R. Strecker (2004), Steady state erosion of critical Coulomb wedges with applications to Taiwan and the Himalaya, *J. Geophys. Res.*, *109*, doi:10.1029/2002JB002284, in press.
- Hilley, G. E., M. R. Strecker, and V. A. Ramos (2004), Growth and erosion of fold-and-thrust belts with an application to the Aconcagua fold-and-thrust belt, Argentina, *J. Geophys. Res.*, *109*, doi:10.1029/2002JB002282, in press.
- Horton, B. K. (1999), Erosional control on the geometry and kinematics of thrust belt development in the central Andes, *Tectonics*, *18*, 1292–1304.
- Hovius, N. (1996), Regular spacing of drainage outlets from linear mountain belts, *Basin Res.*, *8*, 29–44.
- Howard, A. D. (1980), Thresholds in river regimes, in *Thresholds in Geomorphology*, edited by D. R. Coates and J. D. Vitek, pp. 227–258, Allen and Unwin, Concord, Mass.
- Howard, A. D. (1994), A detachment-limited model of drainage basin evolution, *Water Resour. Res.*, *30*, 2261–2285.
- Howard, A. D., and G. Kerby (1983), Channel changes in badlands, *Geol. Soc. Am. Bull.*, *94*, 739–752.
- Howard, A. D., W. E. Dietrich, and M. A. Seidl (1994), Modeling fluvial erosion on regional to continental scales, *J. Geophys. Res.*, *99*, 13,971–13,986.
- Hurtrez, J.-E., F. Lucazeau, J. Lavé, and J.-P. Avouac (1999), Investigation of the relationships between basin morphology, tectonic uplift, and denudation from the study of an active fold belt in the Siwalik Hills, central Nepal, *J. Geophys. Res.*, *104*, 12,779–12,796.
- Jamieson, R. A., and C. Beaumont (1988), Orogeny and metamorphism: A model for deformation and *P-T-T* paths with applications to the central and southern Appalachians, *Tectonics*, *7*, 417–445.
- Keller, E. A., R. L. Zepeda, T. K. Rockwell, T. L. Ku, and W. S. Dinklage (1998), Active tectonics at Wheeler Ridge, southern San Joaquin Valley, California, *Geol. Soc. Am. Bull.*, *110*, 298–310.
- Keller, E. A., D. B. Seaver, D. L. Laduzinsky, D. L. Johnson, and T. L. Ku (2000), Tectonic geomorphology of active folding over buried reverse faults; San Emigdio Mountain front, southern San Joaquin Valley, California, *Geol. Soc. Am. Bull.*, *112*, 86–97.
- Kirby, E., and K. X. Whipple (2001), Quantifying differential rock-uplift rates via stream profile analysis, *Geology*, *29*, 415–418.
- Kirby, E., K. X. Whipple, W. Tang, and Z. Chen (2003), Distribution of active rock uplift along the eastern margin of the Tibetan Plateau: Inferences from bedrock channel longitudinal profiles, *J. Geophys. Res.*, *108*(B4), 2217, doi:10.1029/2001JB000861.
- Kooi, H., and C. Beaumont (1996), Large-scale geomorphology: Classical concepts reconciled and integrated with contemporary ideas via a surface processes model, *J. Geophys. Res.*, *101*, 3361–3386.
- Koons, P. O. (1987), Some thermal and mechanical consequences of rapid uplift: An example for the Southern Alps, New Zealand, *Earth Planet. Sci. Lett.*, *86*, 307–319.
- Koons, P. O. (1989), The topographic evolution of collisional mountain belts: A numerical look at the Southern Alps, New Zealand, *Am. J. Sci.*, *289*, 1041–1069.
- Koons, P. O. (1990), The two-sided orogen: Collision and erosion from the sand box to the Southern Alps, *Geology*, *18*, 679–682.
- Koons, P. O. (1995), Modeling the topographic evolution of collisional belts, *Annu. Rev. Earth Planet. Sci.*, *23*, 375–408.
- Koons, P. O., P. K. Zeitler, C. Chamberlain, D. Craw, and A. S. Meltzer (2002), Mechanical links between erosion and metamorphism in Nanga Parbat, Pakistan Himalaya, *Am. J. Sci.*, *302*, 749–773.
- Lague, D., and P. Davy (2003), Constraints on the long-term colluvial erosion law by analyzing slope-area relationships at various tectonic uplift rates in the Siwalik Hills (Nepal), *J. Geophys. Res.*, *108*(B2), 2129, doi:10.1029/2002JB001893.
- Lavé, J., and J.-P. Avouac (2000), Active folding of fluvial terraces across the Siwalik Hills, Himalayas of central Nepal, *J. Geophys. Res.*, *105*, 5735–5770.
- Lawton, T. F., S. E. Boyer, and J. G. Schmitt (1994), Influence of inherited taper on structural variability and conglomerate distribution, Cordilleran fold and thrust belt, western United States, *Geology*, *22*, 339–342.
- MacGregor, K., R. S. Anderson, S. P. Anderson, and E. D. Waddington (2000), Numerical simulations of glacial-valley longitudinal profile evolution, *Geology*, *28*, 1031–1034.
- Maritan, A., A. Rinaldo, R. Rigon, A. Giacometti, and I. Rodriguez-Iturbe (1996), Scaling laws for river networks, *Phys. Rev. E*, *53*, 1510–1515.
- Masek, J. G., B. L. Isacks, T. L. Gubbels, and E. J. Fielding (1994), Erosion and tectonics at the margins of continental plateaus, *J. Geophys. Res.*, *99*, 13,941–13,956.
- Massong, T. M., and D. R. Montgomery (2000), Influence of sediment supply, lithology, and wood debris on the distribution of bedrock and alluvial channels, *Geol. Soc. Am. Bull.*, *112*, 591–599.
- Merritts, D., and W. B. Bull (1989), Interpreting Quaternary uplift rates at the Mendocino triple junction, northern California, from uplifted marine terraces, *Geology*, *17*, 1020–1024.
- Merritts, D., and K. R. Vincent (1989), Geomorphic response of coastal streams to low, intermediate, and high rates of uplift, Mendocino junction region, northern California, *Geol. Soc. Am. Bull.*, *101*, 1373–1388.
- Molnar, P. (2001), Climate change, flooding in arid environments, and erosion rates, *Geology*, *29*, 1071–1074.
- Molnar, P., and P. England (1990), Late Cenozoic uplift of mountain ranges and global climate change: Chicken or egg?, *Nature*, *346*, 29–34.
- Montgomery, D. R. (1994), Valley incision and the uplift of mountain peaks, *J. Geophys. Res.*, *99*, 13,913–13,921.
- Montgomery, D. R. (2002), Valley formation by fluvial and glacial erosion, *Geology*, *30*, 1047–1050.
- Montgomery, D. R., and M. T. Brandon (2002), Topographic controls on erosion rates in tectonically active mountain ranges, *Earth Planet. Sci. Lett.*, *201*, 481–489.
- Montgomery, D. R., and W. E. Dietrich (1992), Channel initiation and the problem of landscape scale, *Science*, *255*, 826–830.
- Montgomery, D. R., and K. B. Gran (2001), Downstream variations in the width of bedrock channels, *Water Resour. Res.*, *37*, 1841–1846.
- Montgomery, D. R., and H. M. Greenberg (2000), Local relief and the height of Mount Olympus, *Earth Surf. Processes Landforms*, *25*, 385–396.
- Montgomery, D. R., G. Balco, and S. D. Willett (2001), Climate, tectonics, and the morphology of the Andes, *Geology*, *29*, 579–582.
- Montgomery, D. R., N. Finnegan, A. Anders, and B. Hallet (2002), Downstream adjustment of channel width to spatial gradients in rates of rock uplift at Namche Barwa (abstract), *Geol. Soc. Am. Abstr. Programs*, *34*(6), 241.
- Mueller, K., and J. Suppe (1997), Growth of Wheeler Ridge anticline, California: Geomorphic evidence for fault-bend folding behaviour during earthquakes, in *Penrose Conference on Fault-Related Folding*, edited by D. J. Anastasio et al., *Spec. Pap. Geol. Soc. Am.*, *19*, 383–396.
- Pazzaglia, F. J., and M. T. Brandon (1996), Macromorphologic evolution of the post-Triassic Appalachian mountains determined by deconvolution of the offshore basin sedimentary record, *Basin Res.*, *8*, 255–278.
- Pazzaglia, F. J., and M. T. Brandon (2001), A fluvial record of long-term steady-state uplift and erosion across the Cascadia forearc high, western Washington State, *Am. J. Sci.*, *301*, 385–431.
- Rigon, R., I. Rodriguez-Iturbe, A. Maritan, A. Giacometti, D. G. Tarboton, and A. Rinaldo (1996), On Hack's law, *Water Resour. Res.*, *32*, 3367–3374.
- Roe, G. H., D. R. Montgomery, and B. Hallet (2002), Effects of orographic precipitation variations on the concavity of steady-state river profiles, *Geology*, *30*, 143–146.
- Roe, G. H., D. R. Montgomery, and B. Hallet (2003), Orographic precipitation and the relief of mountain ranges, *J. Geophys. Res.*, *108*(B6), 2315, doi:10.1029/2001JB001521.
- Saffer, D. M., and B. A. Bekins (2002), Hydrologic controls on the morphology and mechanics of accretionary wedges, *Geology*, *30*, 271–274.
- Schmidt, K. M., and D. R. Montgomery (1995), Limits to relief, *Science*, *270*, 617–620.
- Sklar, L., and W. E. Dietrich (1998), River longitudinal profiles and bedrock incision models: Stream power and the influence of sediment supply, in *Rivers Over Rock: Fluvial Processes in Bedrock Channels*, *Geophys. Monogr. Ser.*, vol. 107, edited by K. J. Tinkler and E. E. Wohl, pp. 237–260, AGU, Washington, D. C.
- Sklar, L. S., and W. E. Dietrich (2001), Sediment and rock strength controls on river incision into bedrock, *Geology*, *29*, 1087–1090.

- Slingerland, R., S. D. Willett, and H. L. Hennessey (1997), A new fluvial bedrock erosion model based on the work-energy principle, *Eos Trans. AGU*, 78(46), Fall Meet. Suppl., F299.
- Small, E. E., and R. S. Anderson (1995), Geomorphically driven Late Cenozoic rock uplift in the Sierra Nevada, California, *Science*, 270, 277–280.
- Small, E. E., and R. S. Anderson (1998), Pleistocene relief production in Laramide mountain ranges, western United States, *Geology*, 26, 123–126.
- Snyder, N., K. Whipple, G. Tucker, and D. Merritts (2000), Landscape response to tectonic forcing: Digital elevation model analysis of stream profiles in the Mendocino triple junction region, northern California, *Geol. Soc. Am. Bull.*, 112, 1250–1263.
- Snyder, N. P., K. X. Whipple, G. E. Tucker, and D. M. Merritts (2003a), Channel response to tectonic forcing: Analysis of stream morphology and hydrology in the Mendocino triple junction region, northern California, *Geomorphology*, 53, 97–127.
- Snyder, N. P., K. X. Whipple, G. E. Tucker, and D. J. Merritts (2003b), Importance of a stochastic distribution of floods and erosion thresholds in the bedrock river incision problem, *J. Geophys. Res.*, 108(B2), 2117, doi:10.1029/2001JB001655. (Correction, *J. Geophys. Res.*, 108(B8), 2388, doi:10.1029/2003JB002649, 2003)
- Stock, J. D., and W. E. Dietrich (2003), Valley incision by debris flows: Evidence of a topographic signature, *Water Resour. Res.*, 39(4), 1089, doi:10.1029/2001WR001057.
- Suzuki, T. (1982), Rate of lateral planation by Iwaki River, Japan, *Trans. Jpn. Geomorphol. Union*, 3(1), 1–24.
- Tarboton, D. G., R. L. Bras, and I. Rodriguez-Iturbe (1988), The fractal nature of river networks, *Water Resour. Res.*, 24, 1317–1322.
- Tarboton, D. G., R. L. Bras, and I. Rodriguez-Iturbe (1989), Scaling and elevation in river networks, *Water Resour. Res.*, 25, 2037–2051.
- Tomkin, J. H., M. T. Brandon, F. J. Pazzaglia, J. R. Barbour, and S. D. Willett (2003), Quantitative testing of bedrock incision models for the Clearwater River, NW Washington State, *J. Geophys. Res.*, 108(B6), 2308, doi:10.1029/2001JB000862.
- Tucker, G. E. (1996), *Modeling the Large-Scale Interaction of Climate, Tectonics and Topography*, 267 pp., Pa. State Univ. Earth Syst. Sci. Cent., Univ. Park.
- Tucker, G. E. (2004), Drainage basin sensitivity to tectonic and climatic forcing: Implications of a stochastic model for the role of entrainment and erosion thresholds, *Earth Surf. Processes Landforms*, doi:10.1002/esp.1020, 29, 185–205.
- Tucker, G. E., and R. L. Bras (2000), A stochastic approach to modeling the role of rainfall variability in drainage basin evolution, *Water Resour. Res.*, 36, 1953–1964.
- Tucker, G. E., and R. Slingerland (1996), Predicting sediment flux from fold and thrust belts, *Basin Res.*, 8, 329–349.
- Tucker, G. E., and K. X. Whipple (2002), Topographic outcomes predicted by stream erosion models: Sensitivity analysis and intermodel comparison, *J. Geophys. Res.*, 107(B9), 2179, doi:10.1029/2001JB000162.
- van der Beek, P., and P. Bishop (2003), Cenozoic river profile development in the Upper Lachlan catchment (SE Australia) as a test of quantitative fluvial incision models, *J. Geophys. Res.*, 108(B6), 2309, doi:10.1029/2002JB002125.
- Whipple, K. (2001), Fluvial landscape response time: How plausible is steady state denudation?, *Am. J. Sci.*, 301, 313–325.
- Whipple, K. X., and G. E. Tucker (1999), Dynamics of the stream power river incision model: Implications for height limits of mountain ranges, landscape response timescales, and research needs, *J. Geophys. Res.*, 104, 17,661–17,674.
- Whipple, K. X., and G. E. Tucker (2002), Implications of sediment-flux-dependent river incision models for landscape evolution, *J. Geophys. Res.*, 107(B2), 2039, doi:10.1029/2000JB000044.
- Whipple, K., E. Kirby, and S. Brocklehurst (1999), Geomorphic limits to climatically induced increases in topographic relief, *Nature*, 401, 39–43.
- Whipple, K. X., G. S. Hancock, and R. S. Anderson (2000), River incision into bedrock: Mechanics and relative efficacy of plucking, abrasion, and cavitation, *Geol. Soc. Am. Bull.*, 112, 490–503.
- Willett, S. D. (1999a), Orogeny and orography: The effects of erosion on the structure of mountain belts, *J. Geophys. Res.*, 104, 28,957–28,981.
- Willett, S. D. (1999b), Rheological dependence of extension in wedge models of convergent orogens, *Tectonophysics*, 305(4), 419–435.
- Willett, S. D., and M. T. Brandon (2002), On steady states in mountain belts, *Geology*, 30, 175–178.
- Willett, S. D., C. Beaumont, and P. Fullsack (1993), Mechanical model for the tectonics of doubly vergent compressional orogens, *Geology*, 21, 371–374.
- Willett, S. D., R. Slingerland, and N. Hovius (2001), Uplift, shortening, and steady state topography in active mountain belts, *Am. J. Sci.*, 301, 455–485.
- Willgoose, G. (1994), A physical explanation for an observed area-slope-elevation relationship for catchments with declining relief, *Water Resour. Res.*, 30, 151–159.
- Willgoose, G., R. L. Bras, and I. Rodriguez-Iturbe (1991), A coupled channel network growth and hillslope evolution model: 1. Theory, *Water Resour. Res.*, 27, 1671–1684.
- Wobus, C. W., K. Hodges, and K. Whipple (2003), Has focused denudation at the Himalayan topographic front sustained active thrusting near the Main Central Thrust?, *Geology*, 31, 861–864.
- Zhang, P., P. Molnar, and W. R. Downs (2001), Increased sedimentation rates and grain sizes 2–4 Myr ago due to the influence of climate change on erosion rates, *Nature*, 410, 891–897.

B. J. Meade and K. X. Whipple, Department of Earth, Atmospheric and Planetary Sciences, Room 54-1016, Massachusetts Institute of Technology, Cambridge, MA 02139, USA. (meade@mit.edu; kxw@mit.edu)